



Executive summary

Bayesian tracking of two possible unresolved maneuvering targets

Problem area

This report studies the problem of maintaining tracks of two targets that maneuver in and out formation flight, whereas the sensor and measurement extraction chain produces false and possibly unresolved and missing measurements. If the possibility of unresolved measurements is not modeled then one of the tracks may diverge on false measurements, or the two tracks may coalesce. In order to improve this situation, during a series of studies we have developed exact and novel approximate Bayesian filtering approaches to address this problem. First, we developed a combination of a joint IMM for the joint target maneuver modes with an enhanced version of JPDA that takes coupling between target state estimates into account. We refer to this algorithm as Joint IMM Coupled PDA (JIMMCPDA). Subsequently, for this JIMMCPDA filter we developed an enhanced version which addresses track coalescence avoidance yielding the JIMMCPDA* filter, where the * stands for avoiding track coalescence.

Description of work

The aim of the work is to effectively enhance the IMM/JPDA paradigm to situations of possibly unresolved measurements from two targets that maneuver in and out a formation amidst false measurements. This is accomplished by combining a Gaussian shaped two-target resolution model with a descriptor system approach towards tracking multiple targets from missing and false measurements.

First the considered two target track maintenance problem is defined and formulated as a problem of filtering for a jump-linear descriptor system with identically independently distributed (i.i.d.) stochastic coefficients. Next the exact Bayesian filter recursion is derived. Subsequently equations for the mode-conditional mean and covariance are developed. These equations are on their turn used for the development of the Joint interacting Multiple Model Coupled Probabilistic Data Association with Resolution (JIMMCPDAR) filter and a track-coalescence-avoiding version, which is referred to as the JIMMCPDAR*.

Report no.

NLR-TP-2006-693

Author(s)

H.A.P. Blom, E.A. Bloem

Report classification

Unclassified

Date

September 2006

Knowledge area(s)

Advanced (sensor-) information processing

Descriptor(s)

Bayesian estimation
 Descriptor system
 False measurements
 Formation flight
 Markov chain
 Missing measurements
 Multitarget tracking
 Stochastic hybrid system
 Sudden maneuvers
 Unresolved measurements

Results and conclusions

Monte Carlo simulation results of the filters for the problem of tracking two targets that maneuver in and out formation flight, show a significant advantage of the JIMMCPDAR* filter which takes both limited resolution and track coalescence avoidance into account.

Applicability

The applicability of the work comprises the implementation of the JIMMCPDAR* filter in a multitarget tracker, in particular ARTAS, yielding a significant performance improvement for tracking targets that maneuver in close approach situations.



NLR-TP-2006-693

Bayesian tracking of two possible unresolved maneuvering targets

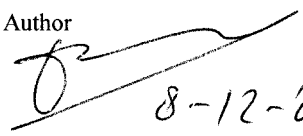
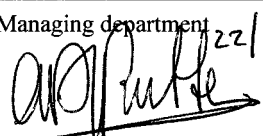
H.A.P. Blom and E.A. Bloem

This report contains a publication to appear in IEEE Tr. Aerospace and Electronic Systems.

This report may be cited on condition that full credit is given to NLR and the authors.

Customer: National Aerospace Laboratory NLR
Working Plan number: 2005 AT.1.C
Owner: National Aerospace Laboratory NLR
Division: Air Transport
Distribution: Unlimited
Classification title: Unclassified
September 2006

Approved by:

Author  8-12-06	Reviewer Anonymous peer reviewers	Managing department  22/12/06
--	--------------------------------------	--

Bayesian tracking of two possibly unresolved maneuvering targets

Henk A.P. Blom & Edwin A. Bloem
National Aerospace Laboratory NLR
Amsterdam, The Netherlands

Abstract

The paper studies the problem of maintaining tracks of two targets that may maneuver in and out formation flight, whereas the sensor and measurement extraction chain produces false and possibly unresolved or missing measurements. If the possibility of unresolved measurements is not modelled than it is quite likely that either the two tracks coalesce or that one of the two tracks diverges on false measurements. In literature a robust measurement resolution model has been incorporated within an IMM/MHT track maintenance setting. A straightforward incorporation of the same model within an IMM and PDA-like hypothesis merging approach suffers from track coalescence. In order to improve this situation, the paper develops a track-coalescence avoiding hypotheses merging version for the two target problem considered. Through Monte Carlo simulations, the novel filters are compared to applying hypotheses merging approaches that ignore the possibility of unresolved measurements or track-coalescence.

Keywords: Bayesian estimation, Descriptor system, False measurements, Formation flight, Markov chain, Missing measurements, Multitarget tracking, Stochastic hybrid system, Sudden maneuvers, Unresolved measurements

I. INTRODUCTION

Daum [1],[2] has well explained that, for closely spaced targets, the probability of resolution typically is worse than the probability of correct measurement association. Hence, the problem of possibly unresolved measurements plays a key role when two targets maneuver in and out of a formation flight amidst false measurements. If the possibility of unresolved measurements is not modelled then one of the tracks may diverge on false measurements, or the two tracks may coalesce. In literature there are a few papers that develop resolution models and incorporate them into effective track maintenance filter equations. Chang & Bar-Shalom [3] introduces a hard measurement distance threshold model regarding yes/no resolution, and incorporates the corresponding error function density within JPDA for two targets. The scenarios considered do not

involve targets that maneuver in and out formation flights. Mori et al. [4] incorporate this error function model within Multiple Hypothesis Tracking (MHT) for non-maneuvering targets. Koch and VanKeuk [5] introduces a Gaussian shaped measure for the probability of resolution for two targets, and shows that this combines smoothly and effectively with MHT for non-maneuvering targets. Koch [6],[7] combines the resolution-MHT with IMM for two targets that maneuver in and out formation. Koch [6] also demonstrates that, under appropriate hypothesis management, this approach performs significantly better than the standard IMM/PDA kind of hypothesis merging approximation of the exact Bayesian filter. In [8], particle filters have also been developed to tracking a formation of two or more targets from false and possibly unresolved or missing measurements, but no targets maneuver in or out the formation.

The aim of this paper is to effectively enhance the IMM/JPDA paradigm to situations of possibly unresolved measurements from two targets that maneuver in and out a formation amidst false measurements. This is accomplished by combining the Gaussian shaped two-target resolution model of [5] with the descriptor system approach towards tracking multiple targets from missing and false measurements [9]. The motivation for the development of this novel approach was triggered by the observation Fitzgerald [10] made for the situation of neither missed nor false measurements: JPDA performance significantly improves when of all permutation hypotheses are being pruned except the most probable one. In [9], the descriptor system formulation has been exploited to extend this positive effect of permutation hypotheses pruning to the more general JPDA setting. This resulted into novel tracking filters which were referred to as CPDA, CPDA* and JPDA*, where the * refers to a particular track coalescence avoiding pruning of permutation hypotheses. Subsequent simulations with these filters showed that CPDA* and JPDA* outperform the other filters, whereas CPDA performs comparable to JPDA.

In a series of follow-up studies the descriptor system and permutation pruning approach is extended to situations of suddenly maneuvering targets, including the development of several novel approximate Bayesian filters, i.e.:

- IMMJPDA* [11],[12] prunes particular permutation hypotheses (similar as JPDA*) in a descriptor system version of the IMMJPDA filter [13];

Manuscript received March 11, 2005; revised January 31, 2006 and August 8, 2006; released for publication ...

Refereeing of this contribution was handled by C. Jauffret.

Authors' address: National Aerospace Laboratory NLR, P.O. Box 90502, 1006BM Amsterdam, The Netherlands (phone: +31 20 5113544; fax: +31 20 5113210; e-mail: blom@nlr.nl, bloem@nlr.nl).

- JIMMCPDA [14],[15] is in theory the best IMM/PDA combination for multiple Markov jump linear targets. [†]
- JIMMCPDA* [14],[15] prunes particular permutation hypotheses in JIMMCPDA similar as in CPDA* ;
- Particle filter approximations of the exact Bayesian filter equations [16]-[18].

A comparison of these track maintenance filters through Monte Carlo simulations [11],[12],[14],[15],[18], it has been shown that JIMMCPDA* and IMMJPDA* typically perform much better than JIMMCPDA and IMMJPDA respectively, and also quite well in comparison to a good particle filter implementation of the exact Bayesian filter equations. Apparently the performance loss due to the CPDA or JPDA type of hypotheses merging is significantly corrected by pruning particular permutation hypotheses. These remarkable results, obtained by the descriptor system approach, motivated the start of a study [19] on how to incorporate the two-target resolution model of [5] with JIMMCPDA and JIMMCPDA*. The current article presents and consolidates the results of this study.

This article is organized as follows. Section II defines the two target track maintenance problem considered. Section III formulates this as a problem of filtering for a jump-linear descriptor system with independent identically distributed (i.i.d.) stochastic coefficients. Section IV develops an exact Bayesian filter recursion. Section V develops equations for the mode-conditional mean and covariance. Sections VI and VII develop the JIMMCPDAR and JIMMCPDAR* filters respectively. Section VIII shows the effectiveness of the novel filters through Monte Carlo simulation results. Section IX draws conclusions.

II. THE TWO TARGET TRACK MAINTENANCE PROBLEM

We consider two targets and assume that the state of each target is modelled as a jump linear system:

$$x_t^i = a^i(\theta_t^i)x_{t-1}^i + b^i(\theta_t^i)w_t^i, \quad i=1,2 \quad (1)$$

where x_t^i is the n -vectorial state of the i -th target, θ_t^i is the Markovian switching mode of the i -th target which assumes values from $\mathbb{M} \triangleq \{1, \dots, N\}$ according to a transition probability matrix Π^i , $a^i(\theta_t^i)$ and $b^i(\theta_t^i)$ are $(n \times n)$ - and $(n \times n')$ -matrices and w_t^i is a sequence of independent identically distributed (i.i.d.) standard Gaussian variables of dimension n' with w_t^i and w_t^j independent for all $i \neq j$ and $w_t^i, (x_0^i, \theta_0^i), (x_0^j, \theta_0^j)$ independent for all $i \neq j$. At $t=0$, the density of (x_0^i, θ_0^i) is known for each i , and in general these densities are i -variant.

We assume that a potential measurement originating from target i is also modelled as a jump linear system:

$$z_t^i = h^i(\theta_t^i)x_t^i + g^i(\theta_t^i)v_t^i, \quad i=1,2 \quad (2)$$

where z_t^i is an m -vector, $h^i(\theta_t^i)$ is an $(m \times n)$ -matrix and $g^i(\theta_t^i)$ is an $(m \times m')$ -matrix, and v_t^i is a sequence of i.i.d. standard Gaussian variables of dimension m' with v_t^i and v_t^j independent for all $i \neq j$. Moreover v_t^i is independent of x_0^j and w_t^j for all i, j .

Let $x_t \triangleq \text{Col}\{x_t^1, x_t^2\}$, $\theta_t \triangleq \text{Col}\{\theta_t^1, \theta_t^2\}$, $z_t \triangleq \text{Col}\{z_t^1, z_t^2\}$, $A(\theta_t) \triangleq \text{Diag}\{a^1(\theta_t^1), a^2(\theta_t^2)\}$, $B(\theta_t) \triangleq \text{Diag}\{b^1(\theta_t^1), b^2(\theta_t^2)\}$,

$$G(\theta_t) \triangleq \text{Diag}\{g^1(\theta_t^1), g^2(\theta_t^2)\}, H(\theta_t) \triangleq \text{Diag}\{h^1(\theta_t^1), h^2(\theta_t^2)\}$$

$w_t \triangleq \text{Col}\{w_t^1, w_t^2\}$ and $v_t \triangleq \text{Col}\{v_t^1, v_t^2\}$, then (1)-(2) yield :

$$x_t = A(\theta_t)x_{t-1} + B(\theta_t)w_t \quad (3)$$

$$z_t = H(\theta_t)x_t + G(\theta_t)v_t \quad (4)$$

with A, B, H and G of size $2n \times 2n$, $2n \times 2n'$, $2m \times 2n$ and $2m \times 2m'$ respectively.

The process $\{\theta_t\}$ assumes values from \mathbb{M}^2 according to transition probability matrix $\Pi = [\Pi_{\eta, \theta}]$, which is a function of Π^1 and Π^2 . Several types of mode switching dependencies between two targets can be modelled. If target modes are independent of each other, i.e. $\text{Prob}\{\theta_t^1 = \theta, \theta_t^2 = \eta\} = \text{Prob}\{\theta_t^1 = \theta\}\text{Prob}\{\theta_t^2 = \eta\}$, then

$$\Pi_{\eta, \theta} = \prod_{i=1}^2 \Pi_{\eta^i, \theta^i}^i, \quad \text{for } \eta \in \mathbb{M}^2 \text{ and } \theta \in \mathbb{M}^2. \quad (5.a)$$

If the target modes are equal, i.e. $\theta_t^2 = \theta_t^1$ for all t , then

$$\begin{aligned} \Pi_{\eta, \theta} &= \Pi_{\eta^1, \theta^1}^1, \quad \text{for } \eta^2 = \eta^1 \text{ and } \theta^2 = \theta^1 \\ &= 0, \quad \text{else.} \end{aligned} \quad (5.b)$$

Between independent (5.a) and equal (5.b) target modes, a spectrum of partial mode dependency models exists. The choice of a specific model from this spectrum is a matter of tracking design. When no prior target mode dependency information is available, then independency (5.a) is the default design choice.

If two targets come nearby each other, then there is a non-zero probability of merging. This event of merging or not is represented by a zero-one-valued process κ_t , where $\kappa_t = 1$

[†] In [17] this JIMMCPDA filter was developed under the name JIMMPDA. In [20] a version of this JIMMCPDA is developed under the name IMMJPDA-Coupled filter.

refers to merging, and $\kappa_i = 0$ refers to non-merging. This implies

$$p_{\kappa_i|x_i,\theta}(0|x,\theta) = 1 - p_{\kappa_i|x_i,\theta}(1|x,\theta) \quad (6)$$

The probability that two targets are resolved or not will depend on their relative distance. For zero distance the probability of merging equals unity, whereas for increasing distance the probability of merging converges to zero. In between these two extremes, the precise behaviour of the probability of merging will depend on the specifics of the sensor and of the signal processing applied. In order to capture a large variety of combined sensor/processing characteristics, [5] suggested a Gaussian shape for the merging probability the parameters of which are clearly related to the coefficients in the measurement model. Taking into account the mode dependency of these coefficients in (2), the state-mode conditional merging probability then becomes:

$$\begin{aligned} p_{\kappa_i|x_i,\theta}(1|x,\theta) &= \exp\left\{-\frac{1}{2}\left(h^1(\theta^1)x^1 - h^2(\theta^2)x^2\right)^T R(\theta)^{-1} \cdot \right. \\ &\quad \left. \cdot \left(h^1(\theta^1)x^1 - h^2(\theta^2)x^2\right)\right\} = \\ &= \exp\left\{-\frac{1}{2}x^T H(\theta)^T \begin{bmatrix} I \\ -I \end{bmatrix} R(\theta)^{-1} [I \ : \ -I] H(\theta)x\right\} \end{aligned} \quad (7)$$

where $R(\theta)$ is an $m \times m$ resolution capability matrix:

$$\begin{aligned} R(\theta) &= \left(g^1(\theta^1)rg^1(\theta^1)^T + g^2(\theta^2)rg^2(\theta^2)^T\right) = \\ &= [I \ : \ I]G(\theta)Diag\{r,r\}G(\theta)^T [I \ : \ I]^T \end{aligned} \quad (8)$$

with $r = Diag\{r_1, \dots, r_m\}$ resolution capability scaling parameters; one for each of the m independent measurement error directions.

We also have to specify the measurement model as a function of κ_i . For this we adopt the sub-model in [3],[21] for two targets of equal strength. For $\kappa_i = 0$, we assume that with a non-zero detection probability, P_d^i , the potential measurement z_t^i of equation (2) is observed at moment t , independently per target. For $\kappa_i = 1$, we assume that with probability P_d^0 the merged potential measurement $(z_t^1 + z_t^2)/2$ is observed at moment t , with z_t^i satisfying equation (2). Hence, our model does not use the additional parameter of [5] for the covariance of the error in the merged measurement.

Let F_t denote the number of false measurements at moment t , we assume F_t to be Poisson distributed:

$$\begin{aligned} p_{F_t}(F) &= \frac{(\lambda V)^F}{F!} \exp(-\lambda V), \quad F = 0, 1, 2, \dots \\ &= 0, \quad \text{else} \end{aligned} \quad (9.a)$$

where λ is the spatial density of false measurements and V is the volume of the observed region. Thus λV is the expected number of false measurements in the observed region. We assume that the false measurements are uniformly distributed in the observed region, which means that a column-vector f_t of F_t i.i.d. false measurements has the following density:

$$p_{f_t|F_t}(f|F) = V^{-F} \quad (9.b)$$

Furthermore we assume that the process $\{F_t, f_t\}$ is a sequence of independent vectors, which are independent of $\{x_t\}, \{w_t\}, \{v_t\}$ and of the merging and detection. At moment $t = 1, 2, \dots, T$, a vector observation y_t is made, the components of which consist of F_t false measurements and D_t detected (merged) potential measurements, in an arbitrary order. The total number L_t of measurements is:

$$L_t = D_t + F_t. \quad (9.c)$$

The multi-target track maintenance problem considered is to estimate (x_t, θ_t) from observations $Y_t \triangleq \{y_s; 0 \leq s \leq t\}$, where y_0 represents the initial density of (x_0, θ_0) .

III. DESCRIPTOR SYSTEM FORMULATION

This section largely follows [9] in characterizing the exact relation between the true measurements y_t and the potential measurements z_t . Let $\phi_{i,t}$ be the detection indicator of target i . For $\kappa_i = 0$ it assumes the value 1 with probability $P_d^i > 0$, independently of $\phi_{j,t}$, $j \neq i$, and the value 0 with probability $(1 - P_d^i)$. For $\kappa_i = 1$, with probability $P_d^0 > 0$ the two potential measurements merge to form one true measurement, i.e. $\phi_{i,t} = \frac{1}{2}$ for $i = 1, 2$, and with probability $1 - P_d^0$ the merged potential measurements do not form a true measurement, i.e. $\phi_{i,t} = 0$ for $i = 1, 2$. The resulting detection indicator vector $\phi_t = Col\{\phi_{1,t}, \phi_{2,t}\}$ is a sequence $\{\phi_t\}$ of i.i.d. vectors, and with a κ_i -conditional distribution:

$$\begin{aligned}
P_{\phi_i|\kappa_i}(\phi_i|\kappa_i) &= \prod_{i=1}^2 (1-P_d^i)^{1-\phi_i} (P_d^i)^{\phi_i} \text{ if } \kappa=0, \phi_i \in \{0,1\}^2 \\
&= \prod_{i=1}^2 (1-P_d^0)^{1-\phi_i} (P_d^0)^{\phi_i} \text{ if } \kappa=1, \phi_i \in \left\{ \begin{bmatrix} 0 \\ 0 \end{bmatrix}, \begin{bmatrix} 1 \\ 1 \end{bmatrix} \right\} \\
&= 0 \quad \text{else.} \quad (10)
\end{aligned}$$

Summation over all components of ϕ_i yields

$$D_t = \sum_{i=1}^M \phi_{i,t}. \quad (11)$$

In order to incorporate the detection indicator ϕ_i within an equation that relates y_t to z_t , we define an operator Φ as follows. For an arbitrary vector ϕ' of length M' and having (0,1)-valued components, let $D(\phi') \triangleq \sum_{i=1}^{M'} \phi'_i$, then the operator Φ produces $\Phi(\phi')$ as a (0,1)-valued matrix of size $D(\phi') \times M'$ of which the i th row equals the i th non-zero row of $\text{Diag}\{\phi'\}$, and, if $\phi' = \text{Col}\{\frac{1}{2}, \frac{1}{2}\}$, then $\Phi(\phi') = [\frac{1}{2}, \frac{1}{2}]$.

With this, the vector \tilde{z}_t that contains all target originating measurements, satisfies:

$$\tilde{z}_t = \Phi(\phi_t)z_t \quad \text{if } D_t > 0 \quad (12)$$

where $\Phi(\phi') \triangleq \Phi(\phi') \otimes I_m$, with I_m a unit-matrix of size m and \otimes Kronecker product, i.e.

$$\begin{bmatrix} a & b \\ c & d \end{bmatrix} \otimes I_m \triangleq \begin{bmatrix} aI_m & \vdots & bI_m \\ & \dots & \\ cI_m & \vdots & dI_m \end{bmatrix}$$

We also introduce a zero-one valued $D_t \times L_t$ -matrix process $\{\tilde{\chi}_t\}$ such that

$$\tilde{\chi}_t y_t = \tilde{z}_t \quad \text{if } D_t > 0 \quad (13a)$$

where $\tilde{\chi}_t \triangleq \tilde{\chi}_t \otimes I_m$. The matrix $\tilde{\chi}_t$ does two things: it selects the target measurements and applies a random permutation to these selected measurements, i.e.

$$\tilde{\chi}_t = \chi_t \Phi(\psi_t) \quad \text{if } D_t > 0. \quad (13b)$$

where χ_t is a $D_t \times D_t$ permutation matrix, which is conditionally independent of ϕ_t given D_t , and where $\psi_t = \text{Col}\{\psi_{1,t}, \dots, \psi_{L_t,t}\}$, with $\psi_{i,t} \in \{0,1\}$ the target

(association) indicator at moment t for measurement i , which assumes the value one if measurement i belongs to a detected target and zero if measurement i comes from clutter. ψ_t is conditionally independent of ϕ_t and χ_t given D_t and L_t . Moreover, $\{\chi_t\}$ and $\{\psi_t\}$ are i.i.d. sequences.

Substitution of (4) into (12) and this into (13a) yields:

$$\tilde{\chi}_t y_t = \Phi(\phi_t)H(\theta_t)x_t + \Phi(\phi_t)G(\theta_t)v_t \quad \text{if } D_t > 0 \quad (14)$$

Notice that the size of $\tilde{\chi}_t$ is $D_t m \times L_t m$ and the size of $\Phi(\phi_t)$ is $D_t m \times M m$. Equation (14) is a jump-linear Gaussian descriptor system (e.g. [22]) with stochastic i.i.d. coefficients $\tilde{\chi}_t$ and $\Phi(\phi_t)$. Equations (3), (4), (6) through (11) and (14) capture the filtering problem to be solved in a mathematically well defined system of equations.

IV. EXACT BAYESIAN FILTER EQUATIONS

In this section a Bayesian characterization of the conditional density $p_{x_t, \theta_t | Y_t}(x, \theta)$ is given where Y_t denotes the σ -algebra generated by the initial densities and the measurements up to and including moment t . The characterization is done in two steps. First, we derive equations for the measurement update of the joint conditional density; i.e. characterize $p_{x_t, \theta_t | Y_t}(x, \theta)$ as a function of $p_{x_{t-1}, \theta_{t-1} | Y_{t-1}}(x, \theta)$; this is prepared in Propositions 1 and 2, and completed in Theorem 1. Second, we derive equations for the interaction and prediction of the joint conditional density; i.e. characterize $p_{x_t, \theta_t | Y_{t-1}}(x, \theta)$ as a function of $p_{x_{t-1}, \theta_{t-1} | Y_{t-1}}(x, \theta)$; this is done in Proposition 3.

Following (14), all target to measurement relevant associations and permutations are covered by $(\phi_t, \tilde{\chi}_t)$ -hypotheses with $D_t > 0$. To this set of hypotheses we add one for the situation $D_t = 0$ through the hypothesis $\phi_t = \{0\}^2$ and $\tilde{\chi}_t = \{\}^{L_t}$. Hence, through defining the weights

$$\beta_t(\phi, \kappa, \tilde{\chi}, \theta) \triangleq \text{Prob}\{\phi_t = \phi, \kappa_t = \kappa, \tilde{\chi}_t = \tilde{\chi}, \theta_t = \theta | Y_t\} \quad (15)$$

the law of total probability yields:

$$p_{x_t, \theta_t | Y_t}(x, \theta) = \sum_{\tilde{\chi}, \phi, \kappa} \beta_t(\phi, \kappa, \tilde{\chi}, \theta) p_{x_t | \theta_t, \phi_t, \kappa_t, \tilde{\chi}_t, Y_t}(x | \theta, \phi, \kappa, \tilde{\chi}) \quad (16)$$

Next, proposition 1 characterizes all terms in this summation.

Proposition 1

For any $\phi \in \{0,1\}^2 \cup \left\{ \text{Col}\left\{ \frac{1}{2}, \frac{1}{2} \right\} \right\}$, such that $D(\phi) \triangleq \sum_{i=1}^2 \phi_i \leq L_i$, and any $\tilde{\chi}_t$ matrix realization $\tilde{\chi}$ of size $D(\phi) \times L_t$, the following holds true at instant t :

$$P_{x_t|\theta, \kappa, \phi, \tilde{\chi}_t, Y_t}(x|\theta, \kappa, \phi, \tilde{\chi}) = \frac{P_{\tilde{z}_t|x_t, \theta, \phi}(\tilde{\chi}_t y_t | x_t, \theta, \phi) \cdot P_{x_t|\theta, \kappa, Y_{t-1}}(x|\theta, \kappa)}{F_t(\phi, \kappa, \tilde{\chi}, \theta)} \quad (17)$$

$$\beta_t(\phi, \kappa, \tilde{\chi}, \theta) = F_t(\phi, \kappa, \tilde{\chi}, \theta) \lambda^{(L_t - D(\phi))} \cdot P_{\phi|\kappa_t}(\phi|\kappa) \cdot P_{\kappa_t|\theta_t, Y_{t-1}}(\kappa|\theta) \cdot P_{\theta_t|Y_{t-1}}(\theta)/c_t \quad (18)$$

where $F_t(\phi, \kappa, \tilde{\chi}, \theta)$ and c_t are such that they normalize $P_{x_t|\theta, \kappa, \phi, \tilde{\chi}_t, Y_t}(x|\theta, \kappa, \phi, \tilde{\chi})$ and $\beta_t(\phi, \kappa, \tilde{\chi}, \theta)$ respectively.

Proof: See appendix A.

The proof in appendix A largely follows the proof of [16, Theorem 1] for the situation of sensors providing perfect resolution. However, the resulting eq. (17) differs significantly from the equation under perfect resolution. The key difference lies in the κ_t -conditionality of the last term in the numerator of (17). The characterization of this last term is done in the following proposition.

Proposition 2

The conditional density $P_{x_t|\theta, \kappa_t, Y_{t-1}}(x|\theta, \kappa)$ in Proposition 1 satisfies for $\kappa_t = 0$ and $\kappa_t = 1$ respectively :

$$P_{x_t|\theta, \kappa_t, Y_{t-1}}(x|\theta, 0) = \frac{1}{1 - q_t(\theta)} P_{x_t|\theta, Y_{t-1}}(x|\theta) - \frac{q_t(\theta)}{1 - q_t(\theta)} P_{x_t|\theta, \kappa_t, Y_{t-1}}(x|\theta, 1) \quad (19)$$

$$P_{x_t|\theta, \kappa_t, Y_{t-1}}(x|\theta, 1) = P_{\kappa_t|x_t, \theta_t}(1|x, \theta) P_{x_t|\theta_t, Y_{t-1}}(x|\theta) / q_t(\theta) \quad (20)$$

with:

$$q_t(\theta) = P_{\kappa_t|\theta_t, Y_{t-1}}(1|\theta) \quad (21)$$

Proof: From Bayes' rule we get

$$P_{x_t|\theta, \kappa_t, Y_{t-1}}(x|\theta, \kappa) = \frac{P_{\kappa_t|x_t, \theta_t}(\kappa|x, \theta) P_{x_t|\theta_t, Y_{t-1}}(x|\theta)}{P_{\kappa_t|\theta_t, Y_{t-1}}(\kappa|\theta)}$$

For $\kappa = 1$ this equals equations (20) and (21).

For $\kappa = 0$, substitution of equation (6) and (20) yields

$$P_{x_t|\theta, \kappa_t, Y_{t-1}}(x|\theta, 0) = \frac{P_{x_t|\theta_t, Y_{t-1}}(x|\theta) - P_{\kappa_t|x_t, \theta_t}(1|x, \theta) P_{x_t|\theta_t, Y_{t-1}}(x|\theta)}{P_{\kappa_t|\theta_t, Y_{t-1}}(0|\theta)} = \frac{P_{x_t|\theta_t, Y_{t-1}}(x|\theta) - q_t(\theta) P_{x_t|\theta_t, \kappa_t, Y_{t-1}}(x|\theta, 1)}{1 - P_{\kappa_t|\theta_t, Y_{t-1}}(1|\theta)}$$

which implies (19)

Q.E.D.

Next we complete the recursion with a characterisation of $P_{x_t, \theta_t|Y_{t-1}}(x|\theta)$ in terms of $P_{x_{t-1}, \theta_{t-1}|Y_{t-1}}(x|\theta)$.

Proposition 3

The prediction of $P_{x_{t-1}, \theta_{t-1}|Y_{t-1}}(x, \theta)$ to $P_{x_t, \theta_t|Y_{t-1}}(x, \theta)$ satisfies for $\theta \in \{1, \dots, N\}^2$:

$$P_{x_{t-1}, \theta_{t-1}|Y_{t-1}}(x, \theta) = \sum_{\eta \in \mathbb{M}^2} \Pi_{\eta\theta} P_{x_{t-1}, \theta_{t-1}|Y_{t-1}}(x, \eta) \quad (22)$$

$$P_{x_t, \theta_t|Y_{t-1}}(x, \theta) = \int_{\mathbb{R}^{2n}} P_{x_t|x_{t-1}, \theta_t}(x|x', \theta) P_{x_{t-1}, \theta_{t-1}|Y_{t-1}}(x', \theta) dx' \quad (23)$$

Proof: By law of total probability

$$P_{x_{t-1}, \theta_{t-1}|Y_{t-1}}(x, \theta) = \sum_{\eta \in \mathbb{M}^2} P_{x_{t-1}, \theta_{t-1}|Y_{t-1}}(x, \theta, \eta) = \sum_{\eta \in \mathbb{M}^2} P_{\theta_t|x_{t-1}, \theta_{t-1}, Y_{t-1}}(\theta|x, \eta) P_{x_{t-1}, \theta_{t-1}|Y_{t-1}}(x, \eta)$$

Because θ_t is conditionally independent of (x_{t-1}, Y_{t-1}) given θ_{t-1} , this yields (22). Also by law of total probability

$$P_{x_t, \theta_t|Y_{t-1}}(x, \theta) = \int_{\mathbb{R}^{2n}} P_{x_t, \theta_t, x_{t-1}|Y_{t-1}}(x, \theta, x') dx' = \int_{\mathbb{R}^{2n}} P_{x_t|x_{t-1}, \theta_t}(x|x', \theta) P_{x_{t-1}, \theta_{t-1}|Y_{t-1}}(x', \theta) dx'$$

Because x_t is conditionally independent of Y_{t-1} given (x_{t-1}, θ_{t-1}) , this yields (23). Q.E.D.

Next we use Propositions 1 and 2 to derive the following characterization of the exact Bayesian filter equations.

Theorem 1

The measurement updating of $P_{x_t, \theta_t|Y_{t-1}}(x, \theta)$ to $P_{x_t, \theta_t|Y_t}(x, \theta)$ satisfies, for $\theta \in \mathbb{M}^2$:

$$P_{x_t, \theta_t|Y_t}(x, \theta) = \sum_{\phi, \tilde{\chi}} \beta_t^0(\theta, \tilde{\chi}, \phi) P_{x_t|\theta_t, \tilde{\chi}_t, \phi, Y_t}^{r=0}(x|\theta, \tilde{\chi}, \phi) + \sum_{\phi, \tilde{\chi}} \beta_t^1(\theta, \tilde{\chi}, \phi) P_{x_t|\theta_t, \kappa_t, \tilde{\chi}_t, \phi, Y_t}(x|\theta, 1, \tilde{\chi}, \phi) \quad (24.a)$$

$$\beta_i^\kappa(\theta, \tilde{\chi}, \phi) = \frac{1}{c_i} F_i^\kappa(\theta, \tilde{\chi}, \phi) q_i(\theta)^\kappa \lambda^{(L_i - D(\phi))}. \quad (24.b)$$

$$\cdot \left[p_{\phi|k_i}(\phi|\kappa) - \kappa p_{\phi|k_i}(\phi|0) \right] p_{\theta|Y_{i-1}}(\theta)$$

$$p_{x_i|\theta_i, \tilde{\chi}_i, \phi_i, Y_i}^{r=0}(x|\theta, \tilde{\chi}, \phi) = \frac{p_{\tilde{z}_i|x_i, \theta_i, \phi_i}(\tilde{\chi} y_i | x, \theta, \phi) p_{x_i|\theta_i, Y_{i-1}}(x|\theta)}{F_i^0(\theta, \tilde{\chi}, \phi)} \quad (24.c)$$

$$p_{x_i|\theta_i, \kappa_i, \tilde{\chi}_i, \phi_i, Y_i}(x|\theta, 1, \tilde{\chi}, \phi) = \frac{p_{\tilde{z}_i|x_i, \theta_i, \phi_i}(\tilde{\chi} y_i | x, \theta, \phi) p_{x_i|\theta_i, \kappa_i, Y_{i-1}}(x|\theta, 1)}{F_i^1(\theta, \tilde{\chi}, \phi)} \quad (24.d)$$

$$p_{\tilde{z}_i|x_i, \theta_i, \phi_i}(\tilde{\chi} y_i | x, \theta, \phi) = N\left\{ \tilde{\chi} y_i; \underline{\Phi}(\phi) H(\theta) x, \underline{\Phi}(\phi) G(\theta) G(\theta)^T \underline{\Phi}(\phi)^T \right\} \quad (24.e)$$

with $p_{x_i|\theta_i, \kappa_i, Y_{i-1}}(x|\theta, 1)$ and $q_i(\theta)$ satisfying (20) and (21) respectively, $F_i^0(\theta, \tilde{\chi}, \phi)$ and $F_i^1(\theta, \tilde{\chi}, \phi)$ normalization functions, and c_i such that $\sum_{\theta, \kappa, \phi, \tilde{\chi}} \beta_i^\kappa(\theta, \chi, \phi) = 1$.

Proof of Theorem 1 : see Appendix B.

By using Theorem 1 and Propositions 2 and 3, we get an exact Bayesian filter recursion which consists of the following steps :

1. Start with $p_{x_{i-1}, \theta_{i-1}|Y_{i-1}}(x|\theta)$ and novel observation y_i ;
2. Equations (22) and (23) yield $p_{x_i, \theta_i|Y_{i-1}}(x|\theta)$;
3. For $p_{\theta_i|Y_{i-1}}(\theta) > 0$ we use

$$p_{x_i|\theta_i, Y_{i-1}}(x|\theta) = p_{x_{i-1}, \theta_{i-1}|Y_{i-1}}(x, \theta) / p_{\theta_i|Y_{i-1}}(\theta) ;$$

4. Equation (20) yields $p_{x_i|\theta_i, \kappa_i, Y_{i-1}}(x|\theta, \kappa)$;

5. Equations (24.a-b) and (21) yield $p_{x_i, \theta_i|Y_i}(x, \theta)$.

Set $t := t + 1$, and repeat the cycle starting at step 1.

V. MODE CONDITIONAL MEAN AND COVARIANCE

Having characterised a set of equations for the exact conditional density, our next step is to derive equations for the mode-conditional mean and covariance. As before we do this in two steps. First, we derive equations for the joint-mode-conditional mean and covariance of the interaction and prediction steps in Proposition 3. Second we use Theorem 1 to derive the measurement update equations for

the joint-mode-conditional mean and covariance under the assumption that the predicted joint target state has a density $p_{x_i, \theta_i, Y_{i-1}}(x|\theta)$ which is Gaussian for each joint θ .

Proposition 4

For each $\theta \in \{1, \dots, N\}^2$, let $\hat{x}_{i-1}(\theta)$ and $\hat{P}_{i-1}(\theta)$ denote the first and second central moments of $p_{x_{i-1}, \theta_{i-1}, Y_{i-1}}(x|\theta)$, and let the solution of

$$p_{\theta_i|Y_{i-1}}(\theta) = \sum_{\eta \in \{1, \dots, N\}^2} \Pi_{\eta, \theta} p_{\theta_{i-1}|Y_{i-1}}(\eta), \quad (25)$$

satisfy $p_{\theta_i|Y_{i-1}}(\theta) > 0$. Then the predicted first and second central moments, $\bar{x}_i(\theta)$ and $\bar{P}_i(\theta)$, of $p_{x_i|\theta_i, Y_{i-1}}(x|\theta)$ satisfy:

$$\bar{x}_i(\theta) = A(\theta) \hat{x}_{i-1|\theta_i}(\theta) \quad (26.a)$$

$$\bar{P}_i(\theta) = A(\theta) \hat{P}_{i-1|\theta_i}(\theta) A(\theta)^T + B(\theta) B(\theta)^T \quad (26.b)$$

where:

$$\hat{x}_{i-1|\theta_i}(\theta) = \sum_{\eta \in \{1, \dots, N\}^m} \Pi_{\eta, \theta} \cdot p_{\theta_{i-1}|Y_{i-1}}(\eta) \cdot \hat{x}_{i-1}(\eta) / p_{\theta_i|Y_{i-1}}(\theta) \quad (27.a)$$

$$\hat{P}_{i-1|\theta_i}(\theta) = \sum_{\eta \in \{1, \dots, N\}^m} \Pi_{\eta, \theta} \cdot p_{\theta_{i-1}|Y_{i-1}}(\eta) \cdot \left(\hat{P}_{i-1}(\eta) + \left[\hat{x}_{i-1}(\eta) - \hat{x}_{i-1|\theta_i}(\theta) \right] \left[\hat{x}_{i-1}(\eta) - \hat{x}_{i-1|\theta_i}(\theta) \right]^T \right) / p_{\theta_i|Y_{i-1}}(\theta) \quad (27.b)$$

Proof of Proposition 4: Eqs. (26.a,b) follow from (23) and (3)'s jump-linearity. Because $p_{\theta_i|Y_{i-1}}(\theta) > 0$, eq. (22) yields

$$p_{x_{i-1}, \theta_{i-1}, Y_{i-1}}(x|\theta) = \sum_{\eta \in \mathbb{M}^2} \Pi_{\eta \theta} p_{x_{i-1}, \theta_{i-1}, Y_{i-1}}(x|\eta) \cdot p_{\theta_{i-1}|Y_{i-1}}(\eta) / p_{\theta_i|Y_{i-1}}(\theta)$$

With this we get :

$$\hat{x}_{i-1|\theta_i}(\theta) = \int x p_{x_{i-1}, \theta_{i-1}, Y_{i-1}}(x|\theta) dx = \sum_{\eta \in \mathbb{M}^2} \Pi_{\eta \theta} \int x p_{x_{i-1}, \theta_{i-1}, Y_{i-1}}(x|\eta) dx \cdot p_{\theta_{i-1}|Y_{i-1}}(\eta) / p_{\theta_i|Y_{i-1}}(\theta)$$

which implies (27.a). Similarly we get (27.b). Q.E.D.

Next we characterize the measurement update equations for the θ_i -conditional mean and covariance, under the assumption that $p_{x_i, \theta_i, Y_{i-1}}(x|\theta)$ is Gaussian for each joint θ .

Theorem 2

For each $\theta \in \mathbb{M}^2$, let $p_{x_i|\theta_i, Y_{i-1}}(x|\theta)$ be Gaussian with mean $\bar{x}_i(\theta)$ and covariance $\bar{P}_i(\theta)$, and let $p_{\theta_i|Y_{i-1}}(\theta) > 0$. Then

$p_{x_i|\theta, Y_i}(x|\theta)$ is a Gaussian mixture, with overall weight $p_{\theta_i|Y_i}(\theta)$, mean $\hat{x}_i(\theta)$ and covariance $\hat{P}_i(\theta)$, satisfying:

$$p_{\theta_i|Y_i}(\theta) = \sum_{\kappa, \phi, \tilde{\chi}} \beta_i^\kappa(\phi, \tilde{\chi}, \theta) \quad (28)$$

$$\hat{x}_i(\theta) = \bar{x}_i(\theta) - \left(\sum_{\phi, \tilde{\chi}} \beta_{i|\theta}^1(\phi, \tilde{\chi}) \right) K_i(\theta) [I: -I] H(\theta) \bar{x}_i(\theta) + \sum_{\substack{\kappa, \phi \\ \phi \neq 0}} K_i^\kappa(\phi, \theta) \left(\sum_{\tilde{\chi}} \beta_{i|\theta}^\kappa(\phi, \tilde{\chi}) \mu_i^\kappa(\phi, \tilde{\chi}, \theta) \right) \quad (29)$$

$$\hat{P}_i(\theta) = \bar{P}_i(\theta) - \left(\sum_{\phi, \tilde{\chi}} \beta_{i|\theta}^1(\phi, \tilde{\chi}) \right) K_i(\theta) [I: -I] H(\theta) \bar{P}_i(\theta) - \sum_{\substack{\kappa, \phi \\ \phi \neq 0}} \left(\sum_{\tilde{\chi}} \beta_{i|\theta}^\kappa(\phi, \tilde{\chi}) \right) K_i^\kappa(\phi, \theta) \underline{\Phi}(\phi) H(\theta) \bar{P}_i^\kappa(\theta) + \sum_{\phi, \tilde{\chi}, \kappa} \beta_{i|\theta}^\kappa(\tilde{\chi}, \phi) \left[\hat{x}_i^\kappa(\theta, \tilde{\chi}, \phi) - \hat{x}_i(\theta) \right] \left[\hat{x}_i^\kappa(\theta, \tilde{\chi}, \phi) - \hat{x}_i(\theta) \right]^T \quad (30)$$

where $\beta_i^\kappa(\phi, \tilde{\chi}, \theta)$ satisfies (24.b), and:

$$\beta_{i|\theta}^\kappa(\phi, \tilde{\chi}) = \beta_i^\kappa(\phi, \tilde{\chi}, \theta) / p_{\theta_i|Y_i}(\theta) \quad (31)$$

$$K_i^\kappa(\phi, \theta) = \bar{P}_i^\kappa(\theta) H(\theta)^T \underline{\Phi}(\phi)^T Q_i^\kappa(\phi, \theta)^{-1} \text{ if } \phi \neq \begin{bmatrix} 0 \\ 0 \end{bmatrix}, \\ = 0 \text{ if } \phi = \begin{bmatrix} 0 \\ 0 \end{bmatrix} \quad (32)$$

$$\bar{x}_i^\kappa(\theta) = \bar{x}_i(\theta) - \kappa K_i(\theta) [I: -I] H(\theta) \bar{x}_i(\theta) \quad (33.a)$$

$$\bar{P}_i^\kappa(\theta) = \bar{P}_i(\theta) - \kappa K_i(\theta) [I: -I] H(\theta) \bar{P}_i(\theta) \quad (33.b)$$

$$K_i(\theta) = \bar{P}_i(\theta) H(\theta)^T \begin{bmatrix} I \\ -I \end{bmatrix} Q_i(\theta)^{-1} \quad (33.c)$$

$$Q_i(\theta) = [I: -I] \left[H(\theta) \bar{P}_i(\theta) H(\theta)^T \right] \begin{bmatrix} I \\ -I \end{bmatrix} + R(\theta) \quad (33.d)$$

$$\mu_i^\kappa(\phi, \tilde{\chi}, \theta) = \tilde{\chi} y_i - \underline{\Phi}(\phi) H(\theta) \bar{x}_i^\kappa(\theta) \quad (34)$$

with :

$$F_i^\kappa(\phi, \tilde{\chi}, \theta) = \exp \left\{ -\frac{1}{2} \mu_i^\kappa(\phi, \tilde{\chi}, \theta)^T Q_i^\kappa(\phi, \theta)^{-1} \mu_i^\kappa(\phi, \tilde{\chi}, \theta) \right\} / \\ \left[(2\pi)^{mD(\phi)} \text{Det}\{Q_i^\kappa(\phi, \theta)\} \right]^{\frac{1}{2}}, \text{ if } \phi \neq \{0\}^2 \quad (35.a) \\ = 1, \text{ if } \phi = \{0\}^2$$

$$Q_i^\kappa(\phi, \theta) = \underline{\Phi}(\phi) (H(\theta) \bar{P}_i^\kappa(\theta) H(\theta)^T + G(\theta) G(\theta)^T) \underline{\Phi}(\phi)^T \quad (35.b)$$

$$q_i(\theta) = \frac{|R(\theta)|^{\frac{1}{2}}}{|Q_i(\theta)|^{\frac{1}{2}}} \cdot \exp \left\{ -\frac{1}{2} \bar{x}_i(\theta)^T H(\theta)^T \begin{bmatrix} I \\ -I \end{bmatrix} Q_i(\theta)^{-1} [I: -I] H(\theta) \bar{x}_i(\theta) \right\} \quad (36)$$

Proof of Theorem 2 : see Appendix C

VI. JOINT IMM COUPLED PDA RESOLUTION FILTER

Proposition 4 and Theorem 2 provide conditional characterizations for the joint targets modes and states. Here we use these equations to specify the JIMMCPDAR filter algorithm (this acronym stands for Joint IMM Coupled PDA Resolution). A filter cycle starts with, for each $\theta \in \mathbb{M}^2$, conditional mode probability $p_{\theta_{-1}|Y_{-1}}(\theta)$ and conditional mean and covariance :

$$\hat{x}_{t-1}(\theta) \triangleq E\{x_{t-1} | \theta_{t-1} = \theta, Y_{t-1}\}, \text{ and}$$

$$\hat{P}_{t-1}(\theta) \triangleq E\{[x_{t-1} - \hat{x}_{t-1}(\theta)][x_{t-1} - \hat{x}_{t-1}(\theta)]^T | \theta_{t-1} = \theta, Y_{t-1}\}$$

One filter cycle consists of the following seven steps.

JIMMCPDAR Step 1: Interaction [23]

Mixes the estimates from the previous filter cycle according to (25) and (27.a,b) in Theorem 2 for each $\theta \in \mathbb{M}^2$:

$$p_{\theta_i|Y_{t-1}}(\theta) = \sum_{\eta \in \mathbb{M}^2} \Pi_{\eta, \theta} \cdot p_{\theta_{-1}|Y_{t-1}}(\eta)$$

$$\hat{x}_{t-1|\theta_i}(\theta) = \sum_{\eta \in \mathbb{M}^2} \Pi_{\eta, \theta} \cdot p_{\theta_{-1}|Y_{t-1}}(\eta) \cdot \hat{x}_{t-1}(\eta) / p_{\theta_i|Y_{t-1}}(\theta)$$

$$\hat{P}_{t-1|\theta_i}(\theta) = \sum_{\eta \in \mathbb{M}^2} \Pi_{\eta, \theta} \cdot p_{\theta_{-1}|Y_{t-1}}(\eta) \cdot \left(\hat{P}_{t-1}(\eta) + \left[\hat{x}_{t-1}(\eta) - \hat{x}_{t-1|\theta_i}(\theta) \right] \left[\hat{x}_{t-1}(\eta) - \hat{x}_{t-1|\theta_i}(\theta) \right]^T \right) / p_{\theta_i|Y_{t-1}}(\theta)$$

JIMMCPDAR Step 2: Prediction

For all $\theta \in \mathbb{M}^2$ evaluate (26.a,b) of Proposition 4:

$$\bar{x}_t(\theta) = A(\theta) \hat{x}_{t-1|\theta_i}(\theta)$$

$$\bar{P}_t(\theta) = A(\theta) \hat{P}_{t-1|\theta_i}(\theta) A(\theta)^T + B(\theta) B(\theta)^T$$

JIMMCPDAR Step 3: Merging prediction :

For all $\theta \in \mathbb{M}^2$ use equations (33.a,b) as approximate equations for the general, non-Gaussian, situation:

$$\bar{x}_t^\kappa(\theta) \triangleq \bar{x}_t(\theta) - \kappa K_i(\theta) [I: -I] H(\theta) \bar{x}_t(\theta)$$

$$\bar{P}_i^{\kappa}(\theta) \equiv \bar{P}_i(\theta) - \kappa K_i(\theta)[I: -I]H(\theta)\bar{P}(\theta)$$

with $K_i(\theta)$ and $Q_i(\theta)$ satisfying (33.c) and (33.d).

JIMMCPDAR Step 4: Gating :

Following [21], now per κ value:

Let $\bar{Q}_i^{\kappa,i}(\theta)$ be the i -th $m \times m$ diagonal block matrix of the κ -conditional predicted $\bar{Q}_i^{\kappa}(\theta)$, with

$$\bar{Q}_i^{\kappa}(\theta) = H(\theta)\bar{P}_i^{\kappa}(\theta)H(\theta)^T + G(\theta)G(\theta)^T \quad (37)$$

Identify for each target i and κ -value the mode $\bar{\theta}_i^{\kappa,i}$ for which $\text{Det}\bar{Q}_i^{\kappa,i}(\theta)$ is largest:

$$\bar{\theta}_i^{\kappa,i} = \underset{\theta}{\text{Argmax}}\{\text{Det}\bar{Q}_i^{\kappa,i}(\theta)\} \quad (38)$$

and identify for each target i a κ -dependent gate $G_i^{\kappa,i} \in \mathbb{R}^m$ as follows:

$$G_i^{\kappa,i} = \left\{ z^i \in \mathbb{R}^m; [z^i - h^i(\bar{\theta}_i^{\kappa,i})\bar{x}_i^{\kappa,i}(\bar{\theta}_i^{\kappa,i})]^T \cdot \bar{Q}_i^{\kappa,i}(\bar{\theta}_i^{\kappa,i})^{-1} \cdot [z^i - h^i(\bar{\theta}_i^{\kappa,i})\bar{x}_i^{\kappa,i}(\bar{\theta}_i^{\kappa,i})] \leq \nu \right\} \quad (39)$$

with ν the gate size. Now we define L_i to denote the number of measurements y_i^j that are in one or more of the gates $G_i^{\kappa,i}$, and $y_i = \text{Col}\{y_i^1, \dots, y_i^{L_i}\}$.

JIMMCPDAR Step 5: Hypothesis evaluation.

Using (24.b) as approximation and adapting the P_d^i and P_d^0 in (10) for reduced detection probability due to limited gate size ν yields:

$$\beta_i^{\kappa}(\phi, \tilde{\chi}, \theta) \equiv F_i^{\kappa}(\phi, \tilde{\chi}, \theta)q_i(\theta)^{\kappa} \lambda^{(L_i - D(\phi))}. \quad (40)$$

$$\begin{cases} \left[p_{\phi_i|\kappa_i}(\phi|\kappa) - \kappa p_{\phi_i|\kappa_i}(\phi|0) \right] p_{\theta_i|y_i}(\theta)/c_i & \text{for } \tilde{\chi} \in \tilde{\mathcal{X}}_i^{\kappa}(\phi) \\ = 0 & \text{for } \tilde{\chi} \notin \tilde{\mathcal{X}}_i^{\kappa}(\phi) \end{cases}$$

$$p_{\phi_i|\kappa_i}(\phi|\kappa) = \prod_{i=1}^2 \left((1 - P_d^i \cdot \text{Chi}_m^2(\nu))^{(1-\phi_i)} (P_d^i \cdot \text{Chi}_m^2(\nu))^{\phi_i} \right) \quad (41)$$

$$\begin{cases} \text{if } \kappa=0, \phi \in \{0,1\}^2 \\ = (1 - P_d^0 \cdot \text{Chi}_m^2(\nu))^{(1-D(\phi))} (P_d^0 \cdot \text{Chi}_m^2(\nu))^{D(\phi)} \\ \text{if } \kappa=1, \phi \in \left\{ \begin{bmatrix} 0 \\ 0 \end{bmatrix}, \begin{bmatrix} 1 \\ 2 \end{bmatrix}, \begin{bmatrix} 0 \\ 1 \end{bmatrix}, \begin{bmatrix} 1 \\ 1 \end{bmatrix} \right\} \\ = 0 & \text{else} \end{cases}$$

with $\text{Chi}_m^2(\cdot)$ the Chi-squared cumulative distribution function with m degrees of freedom, with c_i normalizing $\beta_i^{\kappa}(\phi, \tilde{\chi}, \theta)$, and with $\mu_i^{\kappa}(\phi, \tilde{\chi}, \theta)$, $F_i^{\kappa}(\phi, \tilde{\chi}, \theta)$, $Q_i^{\kappa}(\phi, \theta)$ and $q_i(\theta)$ satisfying (34), (35a,b) and (36) respectively.

JIMMCPDAR Step 6: Measurement-based update, using (28), (29) and (30) as approximations:

$$p_{\theta_i|y_i}(\theta) \equiv \sum_{\kappa, \phi, \tilde{\chi}} \beta_i^{\kappa}(\phi, \tilde{\chi}, \theta)$$

$$\hat{x}_i(\theta) \equiv \bar{x}_i(\theta) - \left(\sum_{\phi, \tilde{\chi}} \beta_{i|\theta}^1(\phi, \tilde{\chi}) \right) K_i(\theta)[I: -I]H(\theta)\bar{x}_i(\theta) + \sum_{\substack{\kappa, \phi \\ \phi \neq 0}} K_i^{\kappa}(\phi, \theta) \left(\sum_{\tilde{\chi}} \beta_{i|\theta}^{\kappa}(\phi, \tilde{\chi}) \mu_i^{\kappa}(\phi, \tilde{\chi}, \theta) \right)$$

$$\hat{P}_i(\theta) \equiv \bar{P}_i(\theta) - \left(\sum_{\phi, \tilde{\chi}} \beta_{i|\theta}^1(\phi, \tilde{\chi}) \right) K_i(\theta)[I: -I]H(\theta)\bar{P}_i(\theta)$$

$$- \sum_{\substack{\kappa, \phi \\ \phi \neq 0}} \left(\sum_{\tilde{\chi}} \beta_{i|\theta}^{\kappa}(\phi, \tilde{\chi}) \right) K_i^{\kappa}(\phi, \theta) \Phi(\phi) H(\theta) \bar{P}_i^{\kappa}(\theta) + \sum_{\phi, \tilde{\chi}, \kappa} \beta_{i|\theta}^{\kappa}(\tilde{\chi}, \phi) \left[\hat{x}_i^{\kappa}(\theta, \tilde{\chi}, \phi) - \hat{x}_i(\theta) \right] \left[\hat{x}_i^{\kappa}(\theta, \tilde{\chi}, \phi) - \hat{x}_i(\theta) \right]^T$$

with $\beta_i^{\kappa}(\phi, \tilde{\chi}, \theta)$, $\beta_{i|\theta}^{\kappa}(\phi, \tilde{\chi})$ and $K_i^{\kappa}(\phi, \theta)$ satisfying (24.b), (31) and (32) respectively.

JIMMCPDAR Step 7: Output equations:

$$\hat{x}_i = \sum_{\theta \in \{1, \dots, N\}^2} p_{\theta_i|y_i}(\theta) \cdot \hat{x}_i(\theta) \quad (42)$$

$$\hat{P}_i = \sum_{\theta \in \{1, \dots, N\}^2} p_{\theta_i|y_i}(\theta) (\hat{P}_i(\theta) + [\hat{x}_i(\theta) - \hat{x}_i] \cdot [\hat{x}_i(\theta) - \hat{x}_i]^T) \quad (43)$$

VII. TRACK-COALESCENCE-AVOIDING JIMMCPDAR FILTER

In [9], the CPDA* filter equations are obtained from the CPDA algorithm by pruning per (ϕ_i, ψ_i) -hypothesis all except the most likely χ_i permutation hypothesis prior to measurement updating. This pruning strategy is a relative simple extension of the effective pruning strategy developed by [10] for JPDA without false or missing measurements. Because for two targets permutations are possible for $\kappa_i = 0$ and $\phi_i = \text{Col}\{1,1\}$ only, we extend the CPDA* hypothesis pruning strategy for that case and for all θ combinations. Hence, for $\kappa=0$ and $\phi = \text{Col}\{1,1\}$ evaluate all (ψ, θ) hypotheses and prune per such (ψ, θ) -hypothesis all except the most likely χ -hypothesis. To do so, define for every ψ and θ a mapping $\hat{\chi}_i(\psi, \theta)$:

$$\hat{\chi}_i(\theta, \psi) \triangleq \underset{\chi}{\text{Argmax}} \beta_i^0(\theta, \chi \Phi(\psi), \text{Col}\{1,1\})$$

with maximization over all permutations χ given $\psi_i = \psi$.

The strategy of evaluating for $\kappa=0$ and $\phi = \text{Col}\{1,1\}$ all (ψ, θ) -hypotheses and only one χ -hypothesis implies that we adopt per $(\phi, \tilde{\chi}, \theta)$ -hypothesis the following hypothesis weights $\hat{\beta}_i^\kappa(\theta, \tilde{\chi}, \phi)$:

$$\begin{aligned} \hat{\beta}_i^\kappa(\theta, \chi \Phi(\psi), \phi) &= \beta_i^\kappa(\theta, \chi \Phi(\psi), \phi) / \hat{c}_i && \text{if } D(\phi) \leq 1, \\ & && \text{or if } D(\phi) = 2 \text{ and } \chi = \hat{\chi}(\theta, \psi) \\ &= 0 && \text{else} \end{aligned} \quad (44)$$

with \hat{c}_i a normalization constant for $\hat{\beta}_i^\kappa$; i.e. such that

$$\sum_{\kappa, \phi, \tilde{\chi}, \theta} \hat{\beta}_i^\kappa(\theta, \tilde{\chi}, \phi) = 1$$

Inserting these particular weights within JIMMCPDAR, yields JIMMCPDAR*, consisting of the following cycle of 8 steps (the first five are equivalent to the first five JIMMCPDAR steps):

JIMMCPDAR* Steps 1-5:

Equivalent to JIMMCPDAR Steps 1-5.

JIMMCPDAR* Step 6: Hypothesis pruning.

First evaluate for every (θ, ψ, ϕ)

$$\hat{\chi}_i(\theta, \psi, \phi) \triangleq \underset{\chi}{\text{Argmax}} \beta_i^0(\theta, \chi^T \Phi(\psi), \phi)$$

Next update all hypothesis weights, using (44):

$$\begin{aligned} \hat{\beta}_i^\kappa(\theta, \chi \Phi(\psi), \phi) &= \beta_i^\kappa(\theta, \chi \Phi(\psi), \phi) / \hat{c}_i && \text{if } D(\phi) \leq 1, \\ & && \text{or if } D(\phi) = 2 \text{ and } \chi = \hat{\chi}(\theta, \psi) \\ &= 0 && \text{else} \end{aligned}$$

with \hat{c}_i a normalization constant for $\hat{\beta}_i^\kappa$; i.e. such that

$$\sum_{\kappa, \phi, \tilde{\chi}, \theta} \hat{\beta}_i^\kappa(\theta, \tilde{\chi}, \phi) = 1$$

JIMMCPDAR* Step 7: Measurement-based update :

Equivalent to JIMMCPDAR Step 6, but with β_i^κ replaced by $\hat{\beta}_i^\kappa$.

JIMMCPDAR* Step 8: Output equations:

Equivalent to JIMMCPDAR Step 7.

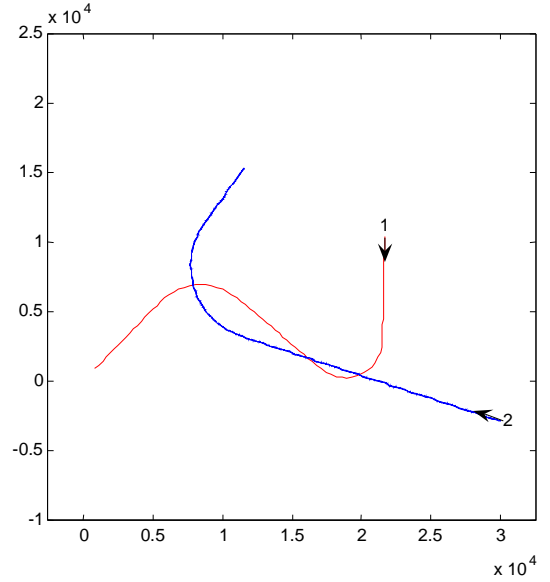


Figure 1: 2D trajectories from [13]

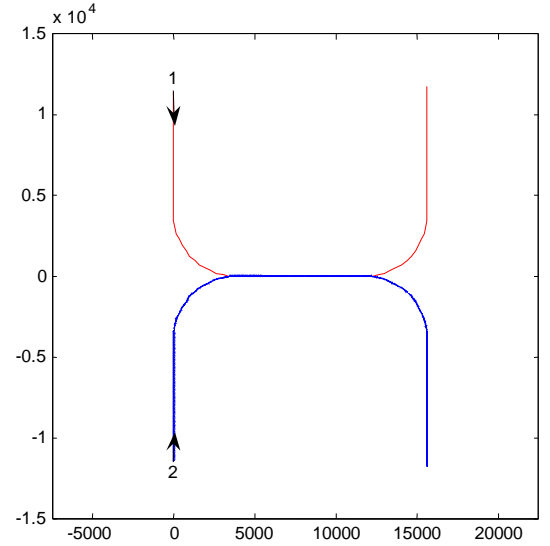


Figure 2: Two targets maneuver in and out formation flight

VIII. MONTE CARLO SIMULATIONS

In this section Monte Carlo simulation results are given for the JIMMCPDAR and JIMMCPDAR* filters and are compared with JIMMCPDA and JIMMCPDA* filters [14],[15]. We consider track maintenance for two targets flying the 2D trajectory patterns as pictured in Figure 1 and in Figure 2. Track initialisation, confirmation or termination is not simulated. The results obtained in this section have initially been presented in [24].

The trajectory pattern in Figure 1 is from [13]. We refer to this as **scenario R0**. In addition to this we consider the scenarios from [14], as depicted in Figure 2, where two targets maneuver in and out formation flight. From 0 to 20s, targets 1 and 2 fly at a speed of 400 m/s in a straight line in south and north direction respectively. From 20 to 35s, both targets make a coordinated turn to the east. From 35 s to 55s, both targets fly in a formation flight in straight line to the east. From 55s to 70s, targets 1 and 2 make a coordinated turn to the north and to the south respectively. From 70s to 90s, targets 1 and 2 fly in a straight line to the north and to the south respectively. Of the trajectories in Figure 2, we consider seven scenarios, which differ in the initial position of Target 1 only:

Scenario R1: Target 1 starts at (0m, 11820m) and target 2 starts at (0m, -11820m). Hence, from 35s to 55s, both targets fly at the same 2D positions.

Scenario R2/R2': Same as R1 but initial position of target 1 is shifted 200m/100m to the south. Hence, from 35s to 55s, target 1 flies 200m/100m south of target 2.

Scenario R3/R3': same as R1 but initial position of target 1 is shifted 200m/100m to the north. Hence, from 35s to 55s, target 1 flies 200m/100m north of target 2.

Scenario R4/R4': Same as R1 but initial position of target 1 is shifted 200/100m to the east. Hence, from 35s to 55s, target 1 flies 200m/100m east of target 2.

For each of the scenarios, Monte Carlo simulations containing 500 runs are performed for each of the tracking filters. In order to make the comparisons more meaningful, for all tracking filters the same random number stream is used.

For each of the tracking algorithms, we assume three possible modes, i.e. $\theta^i \in \{1, 2, 3\}$, with :

Mode 1 (i.e. $\theta^i = 1$): nearly constant velocity with zero mean perturbation in acceleration. The standard deviation of the process noise is $\sigma_a^i(1) = 5m/s^2$.

Mode 2 (i.e. $\theta^i = 2$): Wiener process acceleration (nearly constant acceleration motion). The standard deviation of the process noise is $\sigma_a^i(2) = 7.5m/s^2$.

Mode 3 (i.e. $\theta^i = 3$): Wiener process acceleration (with large acceleration increments, for the onset and termination of manoeuvres). The standard deviation of the process noise is $\sigma_a^i(3) = 40m/s^2$.

The initial mode probabilities for each initial track are assumed to be: [0.8, 0.1, 0.1]. The mode switching probability matrix is assumed to satisfy eq. (5.a) with:

$$\Pi^i = \begin{bmatrix} 0.8 & 0.1 & 0.1 \\ 0.1 & 0.8 & 0.1 \\ 0.1 & 0.1 & 0.8 \end{bmatrix}, \text{ for } i = 1, 2.$$

We adopt this parametrisation in order to assure that none of the trackers uses any advantage of the fact that in scenarios R1/R1' through R4/R4' the targets start and stop maneuvering at the same moments in time.

The target motion model used by the tracking algorithms is from [25]. In each mode the motion dynamics are modeled in Cartesian coordinates, where the state of the target is position, velocity and acceleration in each of the two Cartesian coordinates. Thus x_i^i in (1) has dimension $2n = 6$, and the matrices $a^i(\theta^i)$ and $b^i(\theta^i)$ satisfy,

$$a^i(\theta^i) = \begin{bmatrix} a_1^i(\theta^i) & 0 \\ 0 & a_2^i(\theta^i) \end{bmatrix}, \quad b^i(\theta^i) = \begin{bmatrix} b_1^i(\theta^i) & 0 \\ 0 & b_2^i(\theta^i) \end{bmatrix}$$

$$a_j^i(1) = \begin{bmatrix} 1 & T_s & 0 \\ 0 & 1 & 0 \\ 0 & 0 & 0 \end{bmatrix}, \quad a_j^i(2) = a_j^i(3) = \begin{bmatrix} 1 & T_s & \frac{1}{2}T_s^2 \\ 0 & 1 & T_s \\ 0 & 0 & 1 \end{bmatrix}$$

$$b_j^i(\theta^i) = \sigma_a^i(\theta^i) \cdot \text{Col}\left\{\frac{1}{2}T_s^2, T_s, 0\right\}.$$

The initial track state conditions used are:

$$\hat{x}_0^i(\theta^i) = x_0^i, \quad \theta^i \in \{1, 2, 3\}, i \in \{1, 2\}$$

$$\hat{P}_0^i(\theta) = \text{Diag}\{\hat{P}_0^1(\theta^1), \hat{P}_0^2(\theta^2)\}$$

$$\hat{P}_0^i(\theta^i) = \text{Diag}\{\sigma_1^2, \sigma_2(\theta^i)^2, \sigma_2(\theta^i)^2\}$$

with:

$$\sigma_1 = 20/3, \quad \sigma_2(1) = 5/3, \quad \sigma_2(2) = 2.5, \quad \sigma_2(3) = 40/3$$

Both for the simulated measurements and the tracking filters, the potential sensor measurements for target i are assumed to satisfy eq. (2) with the same coefficients for each θ^i , i.e.

$$h^i(\theta^i) = \begin{bmatrix} h_1^i(\theta^i) & 0 \\ 0 & h_2^i(\theta^i) \end{bmatrix}, \quad g^i(\theta^i) = \begin{bmatrix} g_1^i(\theta^i) & 0 \\ 0 & g_2^i(\theta^i) \end{bmatrix}$$

$$h_j^i(\theta^i) = [1 \ 0 \ 0], \quad g_j^i(\theta^i) = \sigma_m, \quad j \in \{1, 2\}$$

The standard deviation σ_m of the measurement error is $\sigma_m = 20$ m. The sensor is assumed to be located at the coordinate system origin. The sampling interval $T_s = 1$ s and the probability of detection $P_d = 0.997$. False measurements are simulated at a high density of $\lambda = 1 \times 10^{-6} / \text{m}^2 = 1 / \text{km}^2$. The resolution parameter value is $r_1 = r_2 = 10$. The gates for setting up the measurement validation regions are based on the threshold $\nu = 25$.

For each simulation run, we counted track i "O.K.", if

$$|h^i \hat{x}_T^i - h^j x_T^j| \leq 9\sigma_m$$

where $|\cdot|$ denotes the l_2 -norm. We counted track i "Swapped", if track i is not "O.K." and

$$|h^i \hat{x}_T^i - h^j x_T^j| \leq 9\sigma_m \quad \text{for } j \neq i.$$

We counted track i and j as "Coalescing Tracks" if at three or more consecutive observation moments:

$$|h^i \hat{x}_T^i - h^j x_T^j| > 9\sigma_m \quad \wedge \quad |h^i \hat{x}_T^i - h^j \hat{x}_T^j| \leq \sigma_m$$

Using these criteria, the results of the Monte Carlo simulations for the scenarios are depicted in four Tables:

- The percentage of Both tracks "O.K.", in Table 1.
- The percentage of Both tracks "O.K." or "Swapped", in Table 2.
- The percentage of "Coalescing" tracks, in Table 3.
- The average CPU time per scan in Table 4.

Tables 1 through 3 show that JIMMCPDAR* performs much better than JIMMCPDA for all scenarios. The improved performance of JIMMCPDAR* over JIMMCPDA is partly caused by the track coalescence avoidance and partly by taking unresolved measurements into account. The largest impact of sensor resolution modelling applies to those scenarios where the two targets reach each other at 100m distance or less, i.e. R1 (0m), R2' (100m), R3' (100m) and R4' (100m). By comparing the difference with the individual improvements of JIMMCPDA* and JIMMCPDAR over JIMMCPDA, it becomes clear that the two enhancements enforce each other for these scenarios.

Table 1 : % Both tracks 'O.K.'

Scenario	JIMMCPDA	JIMMCPDA*	JIMMCPDAR	JIMMCPDAR*
R0	94.0	94.2	99.2	99.2
R1	0.0	0.0	1.6	11.8
R2	27.4	34.2	28.4	40.2
R2'	0.6	0.2	1.8	31.6
R3	57.2	70.6	65.2	81.4
R3'	1.6	2.4	3.0	40.4
R4	51.8	72.4	63.4	89.4
R4'	0.8	1.6	1.6	42.0

Table 2 : % Both tracks 'O.K.' or both tracks 'Swapped'

Scenario	JIMMCPDA	JIMMCPDA*	JIMMCPDAR	JIMMCPDAR*
R0	94.0	94.2	99.2	99.2
R1	0.0	0.2	3.8	32.0
R2	53.8	69.0	64.8	96.8
R2'	0.8	0.4	3.4	72.2
R3	81.2	89.6	87.2	98.4
R3'	3.0	4.8	9.4	81.6
R4	78.0	89.8	86.2	99.0
R4'	1.4	3.2	3.2	79.8

Table 3 : % Coalescing tracks

Scenario	JIMMCPDA	JIMMCPDA*	JIMMCPDAR	JIMMCPDAR*
R0	0.0	0.0	0.0	0.0
R1	0.0	0.0	36.8	0.2
R2	17.8	0.2	38.0	0.6
R2'	1.0	0.0	76.0	0.0
R3	15.6	0.4	19.8	0.2
R3'	3.8	0.0	73.8	0.0
R4	15.2	0.2	16.6	0.2
R4'	1.4	0.0	82.6	0.0

Table 4 : Average CPU time per scan (in milliseconds)

Scenario	JIMMCPDA	JIMMCPDA*	JIMMCPDAR	JIMMCPDAR*
R0	265	250	361	362
R1	638	620	625	521
R2	375	329	449	342
R2'	638	601	553	411
R3	275	236	378	336
R3'	607	598	525	365
R4	291	226	372	335
R4'	625	608	549	384

Table 5 : % Both tracks ‘O.K.’ under Perfect Resolution

Scenario	JIMMCPDA	JIMMCPDA*	JIMMCPDAR	JIMMCPDAR*
PR0	99.0	99.0	98.8	98.8
PR1	0.6	55.0	1.0	53.2
PR2	80.6	82.2	72.8	72.2
PR2’	9.6	43.8	7.4	43.4
PR3	94.6	97.8	91.2	97.2
PR3’	6.6	31.2	5.4	27.2
PR4	96.6	98.2	94.8	97.6
PR4’	12.4	82.2	10.2	82.2

Table 6 : % Both tracks ‘O.K.’ or both tracks ‘Swapped’ under Perfect Resolution

Scenario	JIMMCPDA	JIMMCPDA*	JIMMCPDAR	JIMMCPDAR*
PR0	99.0	99.0	98.8	98.8
PR1	1.0	99.2	1.2	98.8
PR2	96.4	99.0	94.4	99.2
PR2’	24.8	99.0	16.4	98.2
PR3	96.6	99.2	95.4	99.2
PR3’	26.6	99.2	21.8	99.2
PR4	97.0	98.2	97.0	98.2
PR4’	18.6	98.6	15.6	98.4

Table 7 : % Coalescing tracks under Perfect Resolution

Scenario	JIMMCPDA	JIMMCPDA*	JIMMCPDAR	JIMMCPDAR*
PR0	0.0	0	0.0	0
PR1	99.8	0	99.8	0
PR2	1.6	0	3.0	0
PR2’	49.8	0	61.6	0
PR3	4.6	0	6.8	0
PR3’	55.2	0	58.4	0
PR4	1.2	0	1.2	0
PR4’	69.4	0	76.4	0

Tables 1 and 2 also shows that for all four filters, tracking performance varies significantly with the geometry of how aircraft maneuver in and out formation flight. JIMMCPDAR* performance varies least with these variations.

We also investigated if the novel filters could perform well in case of perfect sensor resolution scenarios. The results of these Monte Carlo simulations are given in Tables 5 through 7. As expected, JIMMCPDA and JIMMCPDA* are now doing much better than in Tables 1 through 3. However, JIMMCPDAR and JIMMCPDAR* also perform significantly better on the perfect resolution scenarios than on the scenarios with unresolved measurements. These results show that the two imperfect resolution filters, which

are based on the measurement model of [5], are far less sensitive to a difference between resolution model and reality than the two perfect resolution filter versions are.

Finally, Table 4 shows that the average computational load is quite similar for all four, and even with JIMMCPDAR* having the best average values.

IX. CONCLUSION

This paper developed exact and approximate Bayesian filter equations to maintaining tracks of two targets maneuvering in and out formation amidst false and possibly unresolved or missing measurements. The limited sensor resolution model of [5] has been incorporated with the descriptor system approach for tracking multiple targets from possibly false and missing measurements [9],[15],[18]. This captures the tracking problem considered into one of filtering for a Markov jump linear descriptor system with stochastic i.i.d. coefficients. For this descriptor system representation exact and approximate Bayesian filter equations have been derived, and two novel tracking algorithms have been developed. These are referred to as Joint IMM Coupled PDA Resolution (JIMMCPDAR) and JIMMCPDAR*, where the * refers to a track-coalescence-avoiding version.

Monte Carlo simulation results of these four filters for the problem of tracking two targets that maneuver in and out formation flight, show a significant advantage of the filter which takes both limited resolution and track coalescence avoidance into account. This corroborates the argumentation by [1], [2] about the high relevance of limited sensor resolution. It also shows that the resolution model of [5] allows the filters to keep on performing well in case the true sensor resolution is better than assumed. Through Monte Carlo simulations it has also been shown that the JIMMCPDAR and JIMMCPDAR* filters perform significantly better than the versions which assume perfect sensor resolution, and that JIMMCPDAR* performs best.

Interesting follow-up research is to compare the performance of the novel filters with those of a good particle filter approximation of our exact recursive Bayesian filter characterization in Section 4. Of complementary interest is to develop a limited resolution version of the approximate tracking filters IMMJPDA and IMMJPDA* [11],[12], and to integrate this with track initiation [26],[27].

The nice results obtained in handling resolution problems when two targets maneuver in and out formation, raise the question how to extend this approach to more than two targets. As a first step, the measurement resolution model needs to be extended to situations of more than two targets. Subsequently these extended resolution models have to be incorporated within the descriptor system formulation and subsequently within the exact and approximate Bayesian filter recursions. For each of these steps, the enhancement involves a systematic enumeration of many more combinations than needed for two targets.

ACKNOWLEDGEMENT

The authors would like to thank anonymous reviewers for their valuable suggestions that were of great help in improving the article.

REFERENCES

1. F.E. Daum, A system approach to multiple target tracking, Ed: Y. Bar-Shalom, Multitarget-Multisensor Tracking: applications and advances, Volume II, Artech House, 1992, pp. 149-181.
2. F.E. Daum, R.J. Fitzgerald, The importance of resolution in multiple target tracking, Proc. SPIE Signal & Data Processing of Small Targets, 1994, Vol. 2238, pp. 329-338.
3. K.C. Chang, Y. Bar-Shalom, Joint Probabilistic Data Association for multitarget tracking with possibly unresolved measurements and maneuvers, IEEE Tr. Automatic Control, Vol. 29 (1984), pp. 585-594.
4. S. Mori et al., Tracking aircraft by acoustic sensors – multiple hypothesis approach applied to possibly unresolved measurements, Proc. ACC, 1987, pp. 1099-1105.
5. W. Koch, G. Van Keuk, Multiple hypothesis track maintenance with possibly unresolved measurements, IEEE Tr. AES, Vol. 33 (1997), pp. 883-892.
6. W. Koch, “On Bayesian MHT for formations with possibly unresolved measurements – Quantitative results, Proc. SPIE, Signal and Data Processing of Small Targets, 1997, Vol. 3163, pp. 417-428.
7. W. Koch, Experimental results on Bayesian MHT for maneuvering closely-spaced objects in a densely cluttered environment, Proc. RADAR1997, IEE, 1997, pp. 729-733.
8. D.J. Salmond and N.J. Gordon, Group tracking with limited sensor resolution and finite field of view, Proc. SPIE Signal & Data Processing of Small Targets, 2000, Vol. 4048, pp. 532-540.
9. H.A.P. Blom, E.A. Bloem, Probabilistic Data Association avoiding track coalescence, IEEE Tr. Automatic Control, Vol. 45 (2000), pp. 247-259.
10. R.J. Fitzgerald, Development of practical PDA logic for multitarget tracking by microprocessor, In: Multitarget-Multisensor Tracking, Advanced Applications, Y. Bar-Shalom (Ed.), Artech House, 1990, pp. 1-23.
11. H.A.P. Blom, E. A. Bloem, “Combining IMM and JPDA for tracking multiple maneuvering targets in clutter,” Proc. 5th Int. Conf. On Information Fusion, July 8-11, 2002, Annapolis, MD, USA, Vol. 1, pp. 705-712.
12. H.A.P. Blom, E. A. Bloem, “Interacting Multiple Model Joint Probabilistic Data Association avoiding track coalescence,” Proc. IEEE Conf. On Decision and Control, 2002, pp. 3408-3415.
13. B. Chen, and J. K. Tugnait, “Tracking of multiple maneuvering targets in clutter using IMM/JPDA filtering and fixed-lag smoothing,” *Automatica*, vol. 37 (2001), pp. 239-249.
14. H.A.P. Blom, E.A. Bloem, Joint IMM and Coupled PDA to track closely spaced targets and to avoid track coalescence, Proc. 7th Int. Conf. on Information Fusion, July 2004, Stockholm, pp. 130-137.
15. H.A.P. Blom, E.A. Bloem, Exact Bayesian filter and joint IMM coupled PDA tracking of maneuvering targets from possibly missing and false measurements, *Automatica*, Vol. 42 (2006), pp. 127-135 and p. 887.
16. H.A.P. Blom, E.A. Bloem, Joint IMPDA Particle filters, Proc. 6th Int. Conf. on Information Fusion, 2003, Vol. 1, pp. 785-792.
17. H.A.P. Blom, E.A. Bloem, Tracking multiple maneuvering targets by Joint combinations of IMM and PDA, Proc. 42nd IEEE Conf. on Decision and Control, 2003, pp. 2965-2970.
18. H.A.P. Blom, E.A. Bloem, Joint particle filtering of multiple maneuvering targets from unassociated measurements, *Journal of Advances in Information Fusion*, Vol. 1 (2006), No. 1, pp. 13-32, at <http://www.isif.org>
19. H.A.P. Blom, E.A. Bloem, Tracking multiple maneuvering targets from possibly unresolved, missing or false measurements, Proc. 7th Int. Conf. on Information Fusion, Philadelphia, July 25-29, 2005.
20. J.K. Tugnait, Tracking of multiple maneuvering targets in clutter using multiple sensors, IMM and JPDA Coupled Filtering, IEEE Tr. AES, Vol. 40 (2004), pp. 320-330.
21. Y. Bar-Shalom, and X. R. Li, “Multitarget-Multisensor Tracking: Principles and Techniques,” *YBS Publishing*, Storrs, CT, 1995.
22. L. Dai, “Singular control systems”, *Lecture notes in Control and information sciences*, Vol. 118, Springer, 1989.
23. H.A.P. Blom, Y. Bar-Shalom, “The Interacting Multiple Model algorithm for systems with Markovian switching coefficients,” *IEEE Trans. Automatic Control*, Vol. 33 (1988), pp. 780-783.
24. H.A.P. Blom, E.A. Bloem, Approximate Bayesian tracking of two targets that maneuver in and out formation flight, Proc. IEEE Int. Conf. on Multisensor Fusion and Integration for intelligent systems, Heidelberg, Germany, 3-6 September 2006.
25. A. Houles, Y. Bar-Shalom, “Multisensor tracking of a maneuvering target in clutter,” *IEEE Tr. Aerospace and Electronic Systems*, Vol. 25 (1989), pp. 176-188.
26. D. Musicki, R.J. Evans, S. Stankovic, Integrated PDA, IEEE Tr. Automatic Control, Vol. 39 (1994), pp. 1237-1241.
27. D. Musicki, R.J. Evans, Integrated Probabilistic Data Association – Finite resolution, *Automatica*, Vol. 31 (1995), pp. 559-570.

APPENDIX A: PROOF OF PROPOSITION 1

First we derive equation (17). If $\phi = 0$ we get

$$P_{x_i|\theta, \kappa, \phi, \tilde{\chi}_i, y_i}(x | \theta, \kappa, 0, \tilde{\chi}) = P_{x_i|\theta, \kappa, y_{i-1}}(x | \theta, \kappa).$$

Else, i.e. for $\phi \neq 0$:

$$\begin{aligned} P_{x_i|\theta, \kappa, \phi, \tilde{\chi}_i, y_i}(x | \theta, \kappa, \phi, \tilde{\chi}) &= \\ &= P_{x_i|\theta, \kappa, \phi, \tilde{\chi}_i, y_i, L_i, y_{i-1}}(x | \theta, \kappa, \phi, \tilde{\chi}, y_i, L_i) = \\ &= P_{x_i|\theta, \kappa, \phi, \tilde{\chi}_i, y_i, L_i, \tilde{z}_i, y_{i-1}}(x | \theta, \kappa, \phi, \tilde{\chi}, y_i, L_i, \tilde{\chi} y_i) = \\ &= P_{x_i|\theta, \kappa, \phi, \tilde{z}_i, y_{i-1}}(x | \theta, \kappa, \phi, \tilde{\chi} y_i) = \\ &= P_{\tilde{z}_i|x_i, \theta, \kappa, \phi, y_{i-1}}(\tilde{\chi} y_i | x, \theta, \kappa, \phi) \cdot \\ &\quad \cdot P_{x_i|\theta, \kappa, \phi, y_{i-1}}(x | \theta, \kappa, \phi) / P_{\tilde{z}_i|\theta, \kappa, \phi, y_{i-1}}(\tilde{\chi} y_i | \theta, \kappa, \phi) = \\ &= P_{\tilde{z}_i|x_i, \theta, \phi}(\tilde{\chi} y_i | x, \theta, \phi) \cdot \\ &\quad \cdot P_{x_i|\theta, \kappa, y_{i-1}}(x | \theta, \kappa) / P_{\tilde{z}_i|\theta, \kappa, \phi, y_{i-1}}(\tilde{\chi} y_i | \theta, \kappa, \phi) \end{aligned}$$

this implies (17) with

$$F_i(\phi, \kappa, \tilde{\chi}, \theta) \triangleq \begin{cases} P_{\tilde{z}_i|\theta, \kappa, \phi, y_{i-1}}(\tilde{\chi} y_i | \theta, \kappa, \phi) & \text{if } \phi \neq \begin{bmatrix} 0 \\ 0 \end{bmatrix} \\ \triangleq 1 & \text{if } \phi = \begin{bmatrix} 0 \\ 0 \end{bmatrix} \end{cases}$$

Subsequently we derive equation (18).

For all $\phi \in \{0, 1\}^2 \cup \text{Col}\{\frac{1}{2}, \frac{1}{2}\}$:

$$\begin{aligned} \beta_i(\phi, \kappa, \tilde{\chi}, \theta) &\triangleq \text{Prob}\{\phi_i = \phi, \kappa_i = \kappa, \tilde{\chi}_i = \tilde{\chi}, \theta_i = \theta | Y_i\} = \\ &= P_{\phi, \kappa, \tilde{\chi}, \theta | Y_i}(\phi, \kappa, \tilde{\chi}, \theta) = \\ &= P_{\phi, \kappa, \tilde{\chi}, \theta | y_i, L_i, y_{i-1}}(\phi, \kappa, \tilde{\chi}, \theta | y_i, L_i) = \\ &= P_{y_i, L_i, \phi, \kappa, \tilde{\chi} | \theta, y_{i-1}}(y_i, L_i, \phi, \kappa, \tilde{\chi} | \theta) P_{\theta | Y_{i-1}}(\theta) / c_i^1 = \\ &= P_{y_i, L_i, \tilde{\chi} | \theta, \phi, \kappa, y_{i-1}}(y_i, L_i, \tilde{\chi} | \theta, \phi, \kappa) \cdot \\ &\quad \cdot P_{\phi, \kappa | \theta, y_{i-1}}(\phi, \kappa | \theta) P_{\theta | Y_{i-1}}(\theta) / c_i^1 = \\ &= P_{y_i, L_i, \tilde{\chi} | \theta, \phi, \kappa, y_{i-1}}(y_i, L_i, \tilde{\chi} | \theta, \phi, \kappa) \cdot \\ &\quad \cdot P_{\phi | \kappa}(\phi | \kappa) P_{\kappa | \theta, y_{i-1}}(\kappa | \theta) P_{\theta | Y_{i-1}}(\theta) / c_i^1 \end{aligned}$$

If $\phi \neq 0$, we have $D_i > 0$ and

$$\tilde{\chi}_i^T \tilde{\chi}_i = \Phi(\psi_i)^T \chi_i \chi_i^T \Phi(\psi_i) = \Phi(\psi_i)^T \Phi(\psi_i) = \text{Diag}\{\psi_i\}$$

Hence $\psi_i = \text{Diag}\{\psi_i\} 1_{L_i} = \tilde{\chi}_i^T \tilde{\chi}_i 1_{L_i}$

with 1_{L_i} an L_i -column vector with 1-valued elements.

Moreover, because

$$\tilde{\chi}_i \Phi(\psi_i)^T = \chi_i^T \Phi(\psi_i) \Phi(\psi_i)^T = \chi_i^T$$

it follows that the transformation from (ψ_i, χ_i) into $\tilde{\chi}_i$ has an inverse. This implies

$$\begin{aligned} P_{y_i, L_i, \tilde{\chi}_i | \theta, \phi, \kappa, y_{i-1}}(y_i, L_i, \chi_i^T \Phi(\psi) | \theta, \phi, \kappa) &= \\ &= P_{y_i, L_i, \psi_i, \chi_i | \theta, \phi, \kappa, y_{i-1}}(y_i, L_i, \psi, \chi | \theta, \phi, \kappa) \end{aligned}$$

Furthermore, because the transformation from (y_i, ψ_i, χ_i) into $(\tilde{z}_i, f_i, \psi_i, \chi_i)$ is a permutation, we get for $L_i > D(\phi) > 0$

$$\begin{aligned} P_{y_i, L_i, \psi_i, \chi_i | \theta, \phi, \kappa, y_{i-1}}(y_i, L_i, \psi, \chi | \theta, \phi, \kappa) &= \\ = P_{\tilde{z}_i, f_i, L_i, \psi_i, \chi_i | \theta, \phi, \kappa, y_{i-1}}(\chi_i^T \Phi(\psi) y_i, \Phi(\psi^*) y_i, L_i, \psi, \chi | \theta, \phi, \kappa) \end{aligned}$$

where $\psi_i^* \triangleq 1 - \psi_i$ for $i = 1, \dots, L_i$.

Hence, for $L_i > D(\phi) > 0$, β_i satisfies :

$$\begin{aligned} \beta_i(\phi, \kappa, \chi_i^T \Phi(\psi), \theta) &= P_{\tilde{z}_i | \theta, \phi, y_{i-1}}(\chi_i^T \Phi(\psi) y_i | \theta, \phi) \cdot \\ &\quad \cdot P_{f_i | \phi, L_i}(\Phi(\psi^*) y_i | \phi, L_i) \cdot P_{\psi_i | \phi, L_i}(\psi | \phi, L_i) P_{\chi_i | \phi}(\chi | \phi) \cdot \\ &\quad \cdot P_{L_i | \phi}(L_i | \phi) P_{\phi | \kappa}(\phi | \kappa) \cdot P_{\kappa | \theta, y_{i-1}}(\kappa | \theta) P_{\theta | Y_{i-1}}(\theta) / c_i^1 \end{aligned}$$

Elaboration of the first five factors and subsequent evaluation of the product of these factors yields :

$$\begin{aligned} \beta_i(\phi, \kappa, \chi_i^T \Phi(\psi), \theta) &= F_i(\phi, \kappa, \chi_i^T \Phi(\psi), \theta) \lambda^{(L_i - D(\phi))} \cdot \\ &\quad \cdot P_{\phi | \kappa}(\phi | \kappa) P_{\kappa | \theta, y_{i-1}}(\kappa | \theta) P_{\theta | Y_{i-1}}(\theta) / c_i \end{aligned}$$

with $c_i = c_i^1 L_i! \exp\{\lambda V\}$, i.e. a normalization constant.

It can easily be verified that the last equation also holds true if $L_i = D(\phi)$ or $D(\phi) = 0$. This yields equation (18).

Q.E.D.

APPENDIX B: PROOF OF THEOREM 1

When $r = 0$ there is always resolution, which implies eq. (24.c). For $\kappa = 1$, equation (17) yields (24.d) with $F_i^1(\theta, \tilde{\chi}, \phi) = F_i(\theta, 1, \tilde{\chi}, \phi)$. Eq. (24.e) follows from (14).

To get (24.a,b) we first substitute (19) into (17) for $\kappa = 0$:

$$P_{x_i|\theta, \kappa, \tilde{\chi}, \phi, Y_i}(x|\theta, 0, \tilde{\chi}, \phi) = p_{\tilde{y}_i|x_i, \theta, \phi}(\tilde{\chi}y_i|x, \theta, \phi) \cdot \left[\frac{p_{x_i|\theta, Y_{i-1}}(x|\theta)}{[1-q_i(\theta)]F_i(\theta, 0, \tilde{\chi}, \phi)} - \frac{q_i(\theta)p_{x_i|\theta, \kappa, Y_{i-1}}(x|\theta, 1)}{[1-q_i(\theta)]F_i(\theta, 0, \tilde{\chi}, \phi)} \right]$$

Next, substituting (24.c) and (24.d) into this and subsequent evaluation yields:

$$\begin{aligned} P_{x_i|\theta, \kappa, \tilde{\chi}, \phi, Y_i}(x|\theta, 0, \tilde{\chi}, \phi) &= \\ &= \frac{F_i^0(\theta, \tilde{\chi}, \phi)}{F_i(\theta, 0, \tilde{\chi}, \phi)} P_{x_i|\theta, \tilde{\chi}, \phi, Y_i}^{r=0}(x|\theta, \tilde{\chi}, \phi) / (1-q_i(\theta)) \\ &\quad - q_i(\theta) \frac{F_i^1(\theta, \tilde{\chi}, \phi)}{F_i(\theta, 0, \tilde{\chi}, \phi)} P_{x_i|\theta, \kappa, \tilde{\chi}, \phi, Y_i}(x|\theta, 1, \tilde{\chi}, \phi) / (1-q_i(\theta)) = \\ &= \frac{1}{1-q_i^1(\theta, \phi, \tilde{\chi})} P_{x_i|\theta, \tilde{\chi}, \phi, Y_i}^{r=0}(x|\theta, \tilde{\chi}, \phi) \\ &\quad - \frac{q_i^1(\theta, \phi, \tilde{\chi})}{1-q_i^1(\theta, \phi, \tilde{\chi})} P_{x_i|\theta, \kappa, \tilde{\chi}, \phi, Y_i}(x|\theta, 1, \tilde{\chi}, \phi) \end{aligned} \quad (\text{H1})$$

$$\text{with: } q_i^1(\theta, \tilde{\chi}, \phi) = \frac{F_i^1(\theta, \tilde{\chi}, \phi)}{F_i^0(\theta, \tilde{\chi}, \phi)} q_i(\theta), \text{ and} \quad (\text{H2})$$

$$F_i(\theta, 0, \tilde{\chi}, \phi) = \frac{F_i^0(\theta, \tilde{\chi}, \phi)}{(1-q_i(\theta))} - q_i(\theta) \frac{F_i^1(\theta, \tilde{\chi}, \phi)}{(1-q_i(\theta))} \quad (\text{H3})$$

Substitution of equation (H1) into equation (16) yields:

$$\begin{aligned} P_{x_i|\theta, Y_i}(x|\theta) &= \sum_{\phi, \tilde{\chi}} \beta_i(\theta, 1, \tilde{\chi}, \phi) p_{x_i|\theta, \kappa, \tilde{\chi}, \phi, Y_i}(x|\theta, 1, \tilde{\chi}, \phi) \\ &\quad + \sum_{\phi, \tilde{\chi}} \frac{\beta_i(\theta, 0, \tilde{\chi}, \phi)}{(1-q_i^1(\theta, \phi, \tilde{\chi}))} P_{x_i|\theta, \tilde{\chi}, \phi, Y_i}^{r=0}(x|\theta, \tilde{\chi}, \phi) \\ &\quad - \sum_{\phi, \tilde{\chi}} \frac{\beta_i(\theta, 0, \tilde{\chi}, \phi) q_i^1(\theta, \phi, \tilde{\chi})}{(1-q_i^1(\theta, \phi, \tilde{\chi}))} P_{x_i|\theta, \kappa, \tilde{\chi}, \phi, Y_i}(x|\theta, 1, \tilde{\chi}, \phi) \end{aligned}$$

which implies (24.a) with:

$$\beta_i^0(\theta, \tilde{\chi}, \phi) = \frac{\beta_i(\theta, 0, \tilde{\chi}, \phi)}{(1-q_i^1(\theta, \phi, \tilde{\chi}))}, \text{ and}$$

$$\beta_i^1(\theta, \tilde{\chi}, \phi) = \beta_i(\theta, 1, \tilde{\chi}, \phi) - \beta_i(\theta, 0, \tilde{\chi}, \phi) \frac{q_i^1(\theta, \phi, \tilde{\chi})}{(1-q_i^1(\theta, \phi, \tilde{\chi}))}$$

Substitution of (18) and subsequent evaluation, using (H2) and (H3), yield:

$$\beta_i^0(\theta, \tilde{\chi}, \phi) = \frac{1}{c_i} F_i^0(\theta, \tilde{\chi}, \phi) \lambda^{(L_i-D(\phi))} p_{\phi|\kappa_i}(\phi|0) p_{\theta_i|Y_{i-1}}(\theta)$$

$$\begin{aligned} \beta_i^1(\theta, \tilde{\chi}, \phi) &= \frac{1}{c_i} F_i^1(\theta, \tilde{\chi}, \phi) q_i(\theta) \lambda^{(L_i-D(\phi))} p_{\phi|\kappa_i}(\phi|1) p_{\theta_i|Y_{i-1}}(\theta) \\ &\quad - \beta_i^0(\theta, \tilde{\chi}, \phi) q_i^1(\theta, \tilde{\chi}, \phi) = \\ &= \frac{1}{c_i} F_i^1(\theta, \tilde{\chi}, \phi) q_i(\theta) \lambda^{(L_i-D(\phi))} p_{\phi|\kappa_i}(\phi|1) p_{\theta_i|Y_{i-1}}(\theta) \\ &\quad - \frac{1}{c_i} F_i^1(\theta, \tilde{\chi}, \phi) q_i(\theta) \lambda^{(L_i-D(\phi))} p_{\phi|\kappa_i}(\phi|0) p_{\theta_i|Y_{i-1}}(\theta) = \\ &= \frac{1}{c_i} F_i^1(\theta, \tilde{\chi}, \phi) q_i(\theta) \lambda^{(L_i-D(\phi))} [p_{\phi|\kappa_i}(\phi|1) - p_{\phi|\kappa_i}(\phi|0)] p_{\theta_i|Y_{i-1}}(\theta) \end{aligned}$$

which implies eq. (24.b). From the above also follows $\sum_{\kappa=0}^1 \beta_i^\kappa(\theta, \tilde{\chi}, \phi) = \sum_{\kappa=0}^1 \beta_i(\theta, \kappa, \tilde{\chi}, \phi)$. Hence c_i normalizes not only $\beta_i(\theta, \kappa, \tilde{\chi}, \phi)$ but also $\beta_i^\kappa(\theta, \tilde{\chi}, \phi)$. Q.E.D.

APPENDIX C: PROOF OF THEOREM 2

The Gaussian assumption and (24.c) imply:

$$P_{x_i|\theta, \tilde{\chi}, \phi, Y_i}^{r=0}(x|\theta, \tilde{\chi}, \phi) = N\{x; \hat{x}_i^0(\theta, \phi, \tilde{\chi}), \hat{P}_i^0(\theta, \phi)\}$$

and completing the square in eq. (24.c) yields:

$$\hat{x}_i^0(\theta, \phi, \tilde{\chi}) = \bar{x}_i(\theta) + K_i^0(\theta, \phi) [\tilde{\chi}y_i - \Phi(\phi)H(\theta)\bar{x}_i(\theta)]$$

$$\hat{P}_i^0(\theta, \phi) = \bar{P}_i(\theta) - K_i^0(\theta, \phi)\Phi(\phi)H(\theta)\bar{P}_i(\theta)$$

with $K_i^0(\theta, \phi)$ satisfying (32), for $\kappa=0$, and where $Q_i^0(\theta, \phi)$ satisfies (35.b).

Equation (20) and the Gaussian assumption yields:

$$P_{x_i|\theta, \kappa, Y_{i-1}}(x|\theta, 1) = N\{x; \bar{x}_i^1(\theta), \bar{P}_i^1(\theta)\},$$

and completing the square in (20) yields eqs. (33.a,b,c,d). Substituting this Gaussian into (17) for $\kappa=1$ yields:

$$P_{x_i|\theta, \kappa, \tilde{\chi}, \phi, Y_i}(x|\theta, 1, \tilde{\chi}, \phi) = N\{x; \hat{x}_i^1(\theta, \tilde{\chi}, \phi), \hat{P}_i^1(\theta, \phi)\}$$

and completing the square in eq. (17) for $\kappa=1$ yields:

$$\hat{x}_i^1(\theta, \phi, \tilde{\chi}) = \bar{x}_i^1(\theta) + K_i^1(\theta, \phi) [\tilde{\chi}y_i - \Phi(\phi)H(\theta)\bar{x}_i^1(\theta)]$$

$$\hat{P}_i^1(\theta, \phi) = \bar{P}_i^1(\theta) - K_i^1(\theta, \phi)\Phi(\phi)H(\theta)\bar{P}_i^1(\theta)$$

with $K_i^1(\theta, \phi)$ satisfying (32), for $\kappa=1$, and where $Q_i^1(\theta, \phi)$ satisfies (35.b)

Normalization of eq. (20) yields

$$q_t(\theta) = \int \exp\left\{-\frac{1}{2}x^T H(\theta)x\right\} \begin{bmatrix} I \\ -I \end{bmatrix} R(\theta)^{-1} [I: -I] H(\theta)x \cdot N\{x; \bar{x}_t(\theta), \bar{P}_t(\theta)\} dx$$

and subsequent evaluation yields (36).

Normalization of eq. (17) for $\kappa=1$, and eq. (24.c) for $r=0$, yields :

$$\begin{aligned} F_t^\kappa(\theta, \tilde{\chi}, \phi) &= \\ &= \int N\{\tilde{\chi}y_t; \underline{\Phi}(\phi)H(\theta)x, \underline{\Phi}(\phi)G(\theta)G(\theta)^T \underline{\Phi}(\phi)^T\} \cdot \\ &\quad \cdot N\{x; \bar{x}_t^\kappa(\theta), \bar{P}_t^\kappa(\theta)\} dx = \\ &= N\{\tilde{\chi}y_t; \underline{\Phi}(\phi)H(\theta)\bar{x}_t^\kappa(\theta), \bar{Q}_t^\kappa(\phi, \theta)\} \end{aligned}$$

with $\bar{x}_t^0(\theta) \triangleq \bar{x}_t(\theta)$ and $\bar{P}_t^0(\theta) \triangleq \bar{P}_t(\theta)$. Subsequent evaluation yields eq. (35.a). From Proposition 1 follows $F_t(\theta, \kappa, \tilde{\chi}, \phi) > 0$ for all $\theta, \kappa, \tilde{\chi}, \phi$. Together with $p_{\theta|Y_{t-1}}(\theta) > 0$ for all θ , eq. (18) yields $\beta_t(\theta, \kappa, \tilde{\chi}, \phi) > 0$ for all $\theta, \kappa, \tilde{\chi}, \phi$. Hence, eq. (15) implies $p_{\theta|Y_t}(\theta) = \sum_{\kappa, \tilde{\chi}} \beta_t(\theta, \kappa, \tilde{\chi}, \phi) > 0$ for all θ . Hence $\beta_{t|\theta}^\kappa(\tilde{\chi}, \phi)$ in eq. (31) is well defined for all $\theta, \kappa, \tilde{\chi}, \phi$. Together with eq. (24.a) this yields:

$$\begin{aligned} \hat{x}_t(\theta) &\triangleq E\{x_t | \theta_t = \theta, Y_t\} = \\ &= \sum_{\phi, \tilde{\chi}} \beta_{t|\theta}^1(\tilde{\chi}, \phi) \hat{x}_t^1(\theta, \tilde{\chi}, \phi) + \sum_{\phi, \tilde{\chi}} \beta_{t|\theta}^0(\tilde{\chi}, \phi) \hat{x}_t^0(\theta, \tilde{\chi}, \phi) \\ \hat{P}_t(\theta) &\triangleq Cov\{x_t | \theta_t = \theta, Y_t\} = \\ &= \sum_{\phi, \tilde{\chi}} \beta_{t|\theta}^1(\tilde{\chi}, \phi) \left[\hat{P}_t^1(\theta, \phi) + [\hat{x}_t^1(\theta, \tilde{\chi}, \phi) - \hat{x}_t(\theta)] [\hat{x}_t^1(\theta, \tilde{\chi}, \phi) - \hat{x}_t(\theta)]^T \right] \\ &+ \sum_{\phi, \tilde{\chi}} \beta_{t|\theta}^0(\tilde{\chi}, \phi) \left[\hat{P}_t^0(\theta, \phi) + [\hat{x}_t^0(\theta, \tilde{\chi}, \phi) - \hat{x}_t(\theta)] [\hat{x}_t^0(\theta, \tilde{\chi}, \phi) - \hat{x}_t(\theta)]^T \right] \end{aligned}$$

Evaluation of $\hat{x}_t(\theta)$ yields :

$$\begin{aligned} \hat{x}_t(\theta) &= \sum_{\kappa, \phi, \tilde{\chi}} \beta_{t|\theta}^\kappa(\tilde{\chi}, \phi) K_t^\kappa(\theta, \phi) \mu_t^\kappa(\theta, \tilde{\chi}, \phi) \\ &+ \bar{x}_t(\theta) \sum_{\phi, \tilde{\chi}} \beta_{t|\theta}^0(\tilde{\chi}, \phi) + \bar{x}_t^1(\theta) \sum_{\phi, \tilde{\chi}} \beta_{t|\theta}^1(\tilde{\chi}, \phi) = \\ &= \bar{x}_t(\theta) + (\bar{x}_t^1(\theta) - \bar{x}_t(\theta)) \left(\sum_{\phi, \tilde{\chi}} \beta_{t|\theta}^1(\tilde{\chi}, \phi) \right) \\ &+ \sum_{\kappa, \phi, \tilde{\chi}} \beta_{t|\theta}^\kappa(\tilde{\chi}, \phi) K_t^\kappa(\theta, \phi) \mu_t^\kappa(\theta, \tilde{\chi}, \phi) = \\ &= \bar{x}_t(\theta) - K_t(\theta) [I: -I] H(\theta) \bar{x}_t(\theta) \left(\sum_{\phi, \tilde{\chi}} \beta_{t|\theta}^1(\tilde{\chi}, \phi) \right) \\ &+ \sum_{\kappa, \phi, \tilde{\chi}} \beta_{t|\theta}^\kappa(\tilde{\chi}, \phi) K_t^\kappa(\theta, \phi) \mu_t^\kappa(\theta, \tilde{\chi}, \phi) \end{aligned}$$

Evaluation of the terms \hat{P}_t^1 and \hat{P}_t^0 in $\hat{P}_t(\theta)$ yields:

$$\begin{aligned} &\sum_{\phi, \tilde{\chi}} \beta_{t|\theta}^1(\tilde{\chi}, \phi) \hat{P}_t^1(\theta, \phi) + \sum_{\phi, \tilde{\chi}} \beta_{t|\theta}^0(\tilde{\chi}, \phi) \hat{P}_t^0(\theta, \phi) = \\ &= \sum_{\phi, \tilde{\chi}} \beta_{t|\theta}^1(\tilde{\chi}, \phi) \left[\bar{P}_t^1(\theta) - K_t^1(\theta, \phi) \underline{\Phi}(\phi) H(\theta) \bar{P}_t^1(\theta) \right] \\ &\quad + \sum_{\phi, \tilde{\chi}} \beta_{t|\theta}^0(\tilde{\chi}, \phi) \left[\bar{P}_t^1(\theta) - K_t^0(\theta, \phi) \underline{\Phi}(\phi) H(\theta) \bar{P}_t^1(\theta) \right] = \\ &= \sum_{\phi, \tilde{\chi}} \beta_{t|\theta}^1(\tilde{\chi}, \phi) \left[\bar{P}_t^1(\theta) - K_t^1(\theta, \phi) [I: -I] H(\theta) \bar{P}_t^1(\theta) \right. \\ &\quad \left. - K_t^1(\theta, \phi) \underline{\Phi}(\phi) H(\theta) \bar{P}_t^1(\theta) \right] \\ &\quad + \sum_{\phi, \tilde{\chi}} \beta_{t|\theta}^0(\tilde{\chi}, \phi) \left[\bar{P}_t^1(\theta) - K_t^0(\theta, \phi) \underline{\Phi}(\phi) H(\theta) \bar{P}_t^1(\theta) \right] = \\ &= \bar{P}_t^1(\theta) - \sum_{\phi, \tilde{\chi}} \beta_{t|\theta}^1(\tilde{\chi}, \phi) K_t^1(\theta, \phi) [I: -I] H(\theta) \bar{P}_t^1(\theta) \\ &\quad - \sum_{\phi} K_t^1(\theta, \phi) \underline{\Phi}(\phi) H(\theta) \bar{P}_t^1(\theta) \left(\sum_{\tilde{\chi}} \beta_{t|\theta}^1(\tilde{\chi}, \phi) \right) \\ &\quad - \sum_{\phi} K_t^0(\theta, \phi) \underline{\Phi}(\phi) H(\theta) \bar{P}_t^1(\theta) \left(\sum_{\tilde{\chi}} \beta_{t|\theta}^0(\tilde{\chi}, \phi) \right) \end{aligned}$$

Substituting this into the eq. for $\hat{P}_t(\theta)$ yields:

$$\begin{aligned} \hat{P}_t(\theta) &= \bar{P}_t^1(\theta) - \sum_{\phi, \tilde{\chi}} \beta_{t|\theta}^1(\tilde{\chi}, \phi) K_t^1(\theta, \phi) [I: -I] H(\theta) \bar{P}_t^1(\theta) \\ &\quad - \sum_{\phi} K_t^1(\theta, \phi) \underline{\Phi}(\phi) H(\theta) \bar{P}_t^1(\theta) \left(\sum_{\tilde{\chi}} \beta_{t|\theta}^1(\tilde{\chi}, \phi) \right) \\ &\quad - \sum_{\phi} K_t^0(\theta, \phi) \underline{\Phi}(\phi) H(\theta) \bar{P}_t^1(\theta) \left(\sum_{\tilde{\chi}} \beta_{t|\theta}^0(\tilde{\chi}, \phi) \right) \\ &+ \sum_{\phi, \tilde{\chi}} \beta_{t|\theta}^1(\tilde{\chi}, \phi) \left[\hat{x}_t^1(\theta, \tilde{\chi}, \phi) - \hat{x}_t(\theta) \right] \left[\hat{x}_t^1(\theta, \tilde{\chi}, \phi) - \hat{x}_t(\theta) \right]^T \\ &+ \sum_{\phi, \tilde{\chi}} \beta_{t|\theta}^0(\tilde{\chi}, \phi) \left[\hat{x}_t^0(\theta, \tilde{\chi}, \phi) - \hat{x}_t(\theta) \right] \left[\hat{x}_t^0(\theta, \tilde{\chi}, \phi) - \hat{x}_t(\theta) \right]^T \end{aligned}$$

Rewriting this yields (30).

Q.E.D.